RS2

2D finite element program for stress analysis and support design
around excavations in soil and rock

Dynamic Module Verification Manual

Table of Contents

1 Natural Period of One-Dimensional Column

1.1 Problem Description

This problem involves wave propagation in a plane-strain soil column with width 1 m and height 10 m subjected to gravity. The mesh is divided into 3-node elements as presented in Figure **1-1**.

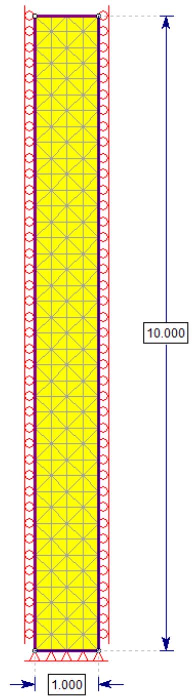

Figure 1-1: Jointed rock column as constructed in RS2

Table 1.1: Input parameters for one-dimensional column model

Parameter	***Value***
Material type	Elastic
Young's modulus (*E*)	50000 kPa
Poisson's ratio (*v*)	0
Unit weight (γ)	20 kN/m^3
Height (*L*)	10.0 m
Width (*w*)	1.0 m

1.2 Analytical Solution

Natural period of an elastic column with one end open and one end close is:

$$T = 4L\sqrt{\frac{\rho}{E}} \tag{1.1}$$

where L is the height of the column, E is the elastic modulus of the column and ρ is the soil mass.

Analytical natural period: T = 0.255 s.

1.3 Results

Figure 1-2 shows the vertical displacement at top of the soil column with time as produced by RS2. The natural period calculated in RS2 is 0.256 s, which agrees well with the analytical solution.

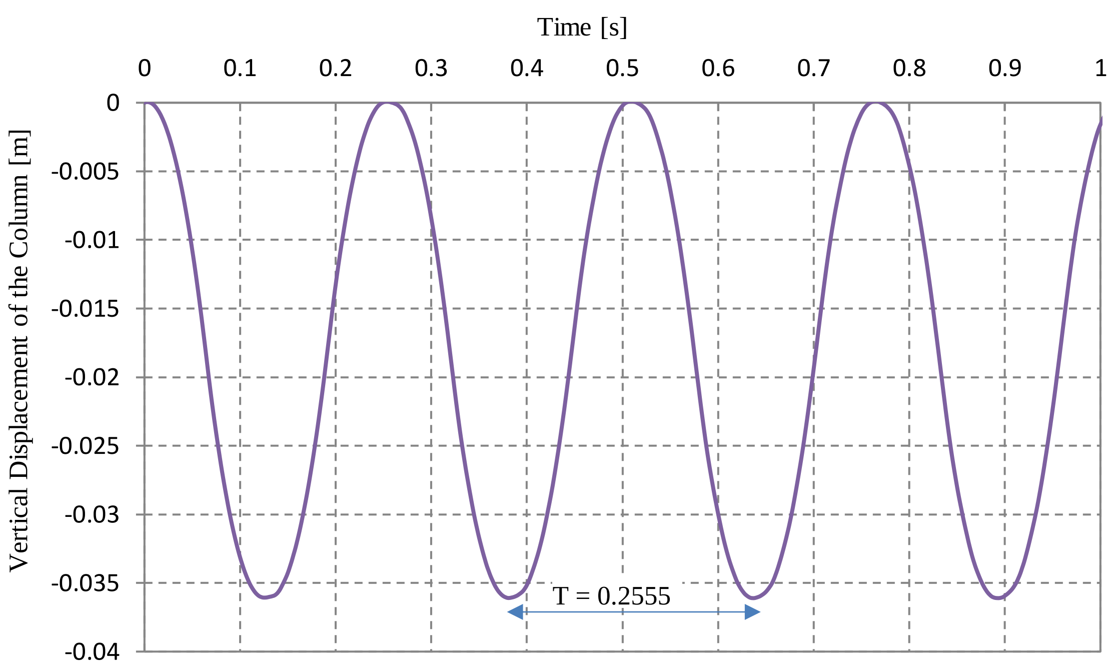

Figure 1-2: RS2 Solution. Vertical Displacements-Time

1.4 References

Itasca Consulting Group (2005). FLAC – Fast Langrangian Analysis of Continua, Version 5, User's Manual. Itasca Consulting Group, Inc, Minneapolis, Minnesota.

1.5 Data Files

The input data file **Dynamic #001.fez** can be downloaded from the RS2 Online Help page for Verification Manuals.

2 Forced Vibration of an Elastic Solid in Plane Strain

2.1 Problem Description

In this problem, an elastic rod with length 10.5 m and height 0.5 m is constrained to vibrate in the axial direction only. The rod is fixed at the right end. The mesh is divided into 3-node elements (see Figure 2-1). A uniform unit velocity at t = 0 is initially applied to all freedoms in the mesh. Displacements close to the support are analyzed.

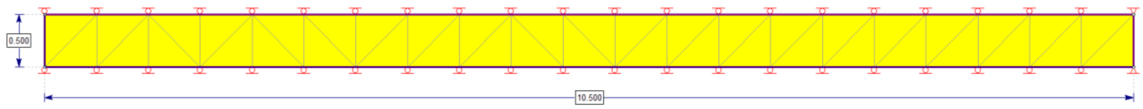

Figure 2-1: RS2 model of an elastic rod

Table 2.1: Model parameters

Parameter	***Value***
Material type	Elastic
Young's modulus (E)	10000 kPa
Poisson's ratio (v)	0.0
Unit weight (γ)	9.81 kN/m^3
Length (L)	10.5 m
Height (w)	0.5 m

2.2 Analytical Solution

Analytical solution for natural period of the rod according to [1] is 0.4 s. The maximum displacement close to the support is 0.005 m. The analytical displacement-time relationship is shown in Figure 2-2.

2.3 Results

The result of RS2 computation is shown in Figure 2-2. RS2 is in close agreement with both the analytical solution and the results obtained from FEM modeling in [1].

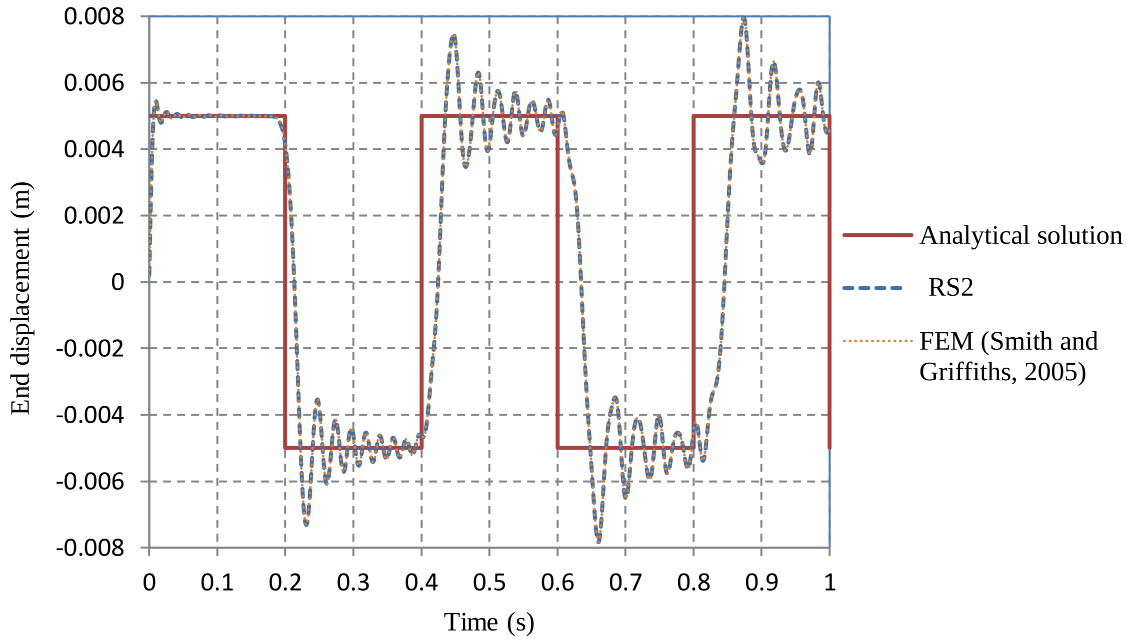

Figure 2-2: Displacements close to the support

2.4 References

Smith, I. M., and Griffiths, D. V. (2004). Programming the finite element method, 4th Ed., Wiley, Chichester, U.K.

2.5 Data Files

The input data file **Dynamic #002.fez** can be downloaded from the RS2 Online Help page for Verification Manuals.

3 Simply Supported Beam with Constant Uniform Loading

3.1 Problem Description

This problem concerns the dynamic behavior of a simply supported beam. The natural period of the beam is determined and compared with analytical solution. In order to obtain the natural period, a distributed load of 10 kN/m/m is applied on the beam. The geometry of the problem is shown in Figure 3-1. Material properties of the beam are shown in Table 3.1.

Figure 3-1: Simply supported beam modeled in RS2

Table 3.1: Model parameters

Parameter	***Value***
Material type	Elastic
Young's modulus (E)	300000 kPa
Unit weight (γ)	9.81 kN/m^3
Length (L)	1.0 m
Thickness (h)	0.1 m

3.2 Analytical Solution

The natural frequency of the first mode of vibration is given by:

$$\omega_n = \pi^2 \sqrt{\frac{EI}{mL^4}} \tag{3.1}$$

where E is the elastic modulus of the beam, I is the moment of inertia, m is the mass per unit of length and L is the length of the beam.

According to equation (3.1), the natural frequency and period of the beam are respectively:

$$\omega_n = 156.05 \text{ (rad/s)} \quad \text{and} \quad T_n = \frac{2\pi}{\omega_n} = 0.0403s$$

Though a continuous beam will have many modes contributing to its dynamic motion, a simply supported beam undergoing a constant uniform load will respond primarily in the fundament period. Consequently, the system will behave similar to a single degree of freedom system under a constant load, even though the beam in reality has a distributed mass along the entirety of the beam. Therefore, the vertical displacement at the center beam is described by the following formula:

$$u_v = \frac{P}{K}\left(1 - \cos\left(\omega_n t\right)\right) \tag{3.2}$$

3.3 Results

Figure 3-2 shows the time-dependent vertical displacement of the beam calculated using RS2. The natural period calculated in RS2 is 0.040 s, and along with the general vertical motion of the beam agrees well with the analytical solution.

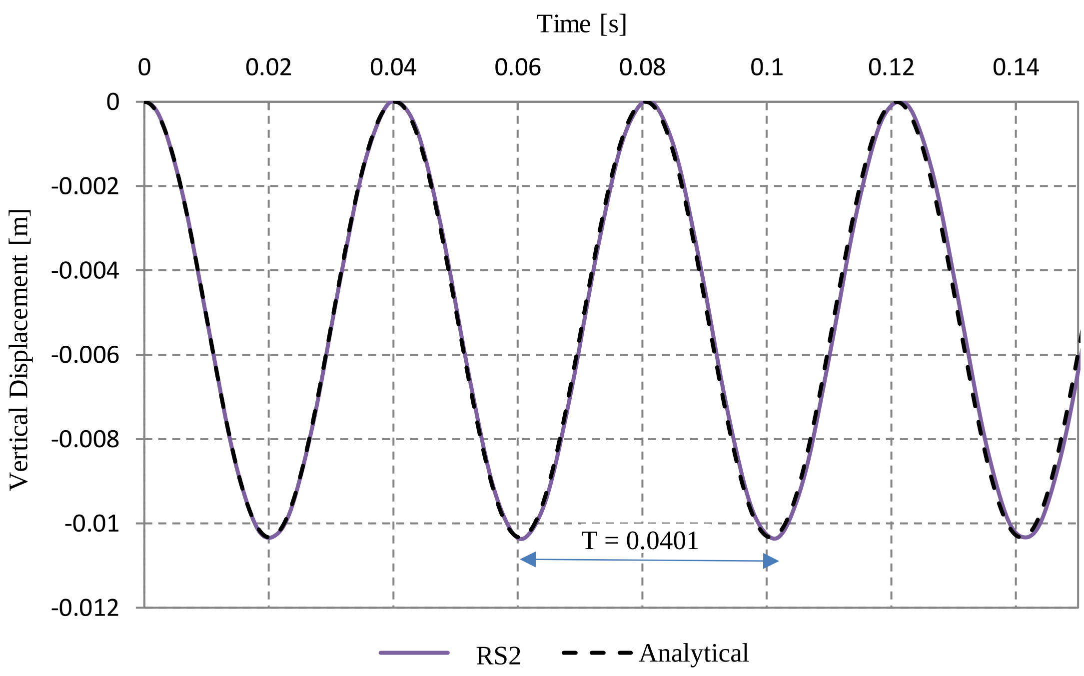

Figure 3-2: RS2 solution of the vertical displacement-time relationship

3.4 References

Brinkgreve, R. B. (2002) Plaxis 2D Version 8.4: Reference, Scientific and Dynamic Manuals, Lisse, Balkema.

3.5 Data Files

The input data file **Dynamic #003.fez** can be downloaded from the RS2 Online Help page for Verification Manuals.

4 Timoshenko Beams Subjected to a Harmonic Point Load

4.1 Problem Description

This problem involves loading a beam model identical to the one in the previous chapter with a point load at midspan that changes amplitude harmonically. Whereas the previous example allowed for the model to behave as a single degree of freedom system, the harmonic load now will excite the beam's higher mode responses. An analytical solution does exist for a simply supported beam for which to compare the results of the RS2 model.

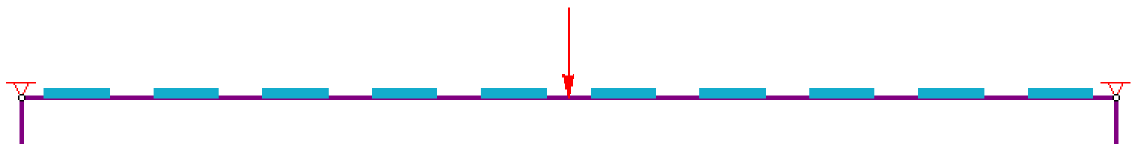

Figure 4-1: Simply supported beam modeled in RS2

Table 4.1: Model parameters

Parameter	*Value*
Material type	Elastic
Young's modulus (E)	300000 kPa
Unit weight (γ)	9.81 kN/m^3
Poisson's Ratio	0
Length (L)	1.0 m
Thickness (h)	0.1 m

The beam is loaded with a harmonic load at the midspan of the beam with an amplitude of 1 kN and a forcing frequency, $\bar{\omega}$, of 40 Hz.

4.2 Analytical Solution

Any number of natural frequencies of the beam may be calculated using Eq. (4.1), where *n* is the number of the mode number.

$$\omega_n = \frac{n^2\pi^2}{L^2}\sqrt{\frac{EI}{m}} \tag{4.1}$$

Each of these frequencies corresponds to a unique modal response that contributes to the overall response of the beam that is being subjected to the harmonic point load. The analytical solution may be determined by calculating the modal responses of the beam and the sum of these responses will be the overall response of the beam since the beam is modelled linear-elastically. Eq. (4.2) is the analytical solution to the simply supported beam.

Each mode's dynamic response can be described by the response of an equivalent undamped single degree of freedom system's response to a harmonic load, with parameters determined from the mode's natural frequency. The expression within the square brackets of Eq. (4.2) contains the response function of the equivalent single degree of freedom system.

$$u(x,t) = \frac{2PL^3}{\pi^4 EI}\sum_{n=0}^{\infty}\frac{\phi\left(\frac{L}{2}\right)}{n^4}\left[R_n \sin(\overline{\omega}t-\theta) - \frac{\beta_n}{1-\beta_n{}^2}\sin\omega_n t\right]\sin\left(\frac{n\pi x}{L}\right) \tag{4.2}$$

Where:

$$\beta_n = \overline{\omega}/\omega_n$$

$$R_n = \frac{\beta_n}{\left|1-\beta_n{}^2\right|}$$

$$\theta = \begin{cases} 0, & \beta_n < 0 \\ \pi, & \beta_n > 0 \end{cases}$$

The ϕ function describes the shape of the beam for each mode. The mode shapes of the beam correspond to sinusoidal curves with half-periods that are fractions of the length of the total beam. The shape function is included in Eq. (4.2) as the final sinusoid expression that is dependent on *x*, distance along the beam, rather than time. At the midspan there exists only three options for the value of this function as described below:

$$\phi(L/2) = \begin{cases} 0 & n = 2,4,6,\ldots \\ 1 & n = 1,5,9,\ldots \\ -1 & n = 3,7,11,\ldots \end{cases}$$

The contribution of each mode needs to be determined and then summed together to determine the overall response of the system analytically.

4.3 Results

Figure 4-2 shows the time-dependent vertical displacement of the beam calculated using RS2. The initial response of the model corresponds well with the analytical solution but beyond the 0.1 s mark there is visible amplitude reduction occurring. This is most likely due to integration scheme's propensity to reduce a response's amplitude.

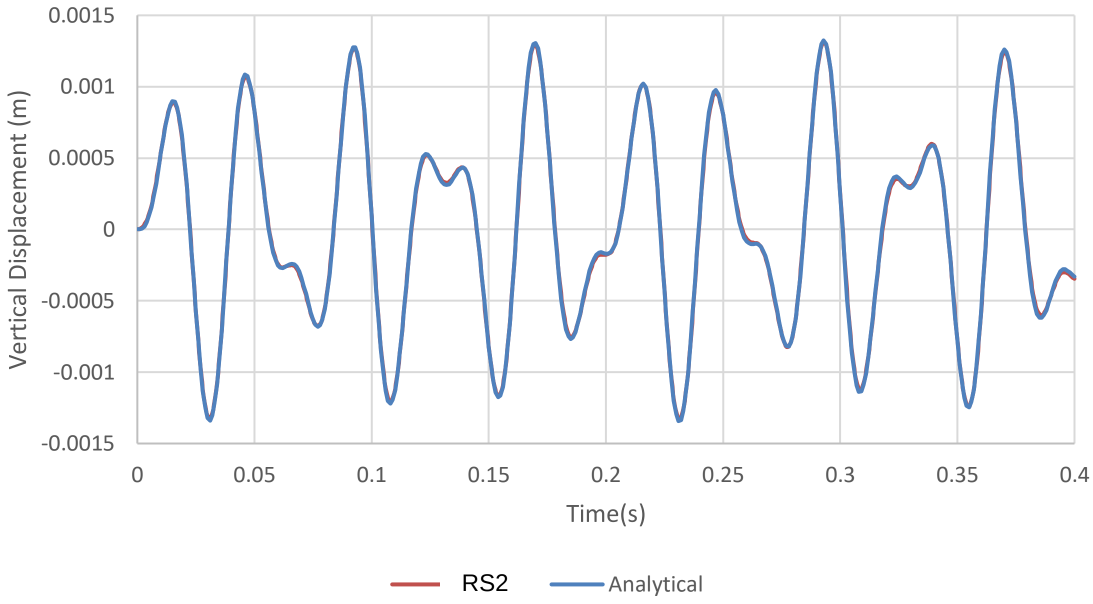

Figure 4-2: RS2 solution of the vertical displacement-time relationship

4.4 References

Chopra, A. K. (1995). *Dynamics of Structures*. New Jersey: Prentice Hall.

4.5 Data Files

The input data file **Dynamic #004.fez** can be downloaded from the RS2 Online Help page for Verification Manuals.

5 Simply Supported Beam Subjected to a Harmonic Point Load

5.1 Problem Description

This problem will model the same problem system as Chapter 4 by using plane strain quadrilateral elements rather than linear beam elements using Timoshenko beam theory. The results of this analysis should be similar if not even more accurate than the previous analysis.

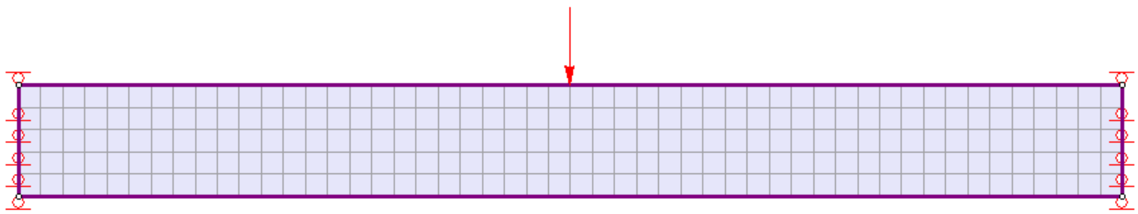

Figure 5-1 Simply Supported Beam Modeled in RS2

The problem is using the same parameters that are listed in Table 4.1.

5.2 Analytical Solution

The analytical solution provided in Section 4.2 accounts solely for deflection in the beam arising from bending and ignores shear deformations. The majority of the displacement may be contributed by the beam bending in static analysis, however in dynamic analysis accounting for shear deformation will lower the natural frequencies of the system and alter the response. Using a greater number of elements in the RS2 model will presumably capture the effect of shear deformation on the beam's dynamic response better.

The shortening of the frequency is described in Eq. (5.1).

$$\omega'_n = \omega_n \left[1 + \left(\frac{n\pi r}{L}\right)^2 \left(1 + \frac{E}{\kappa G}\right)\right]^{-0.5} \tag{5.1}$$

Where r denotes the modulus of gyration is equal to the square root of the ratio between a cross section's second moment of area and its area.

$$r = \sqrt{\frac{I}{A}} \tag{5.2}$$

G is the shear modulus of the beam and κ is the Timoshenko shear coefficient, a correction parameter introduced to account for non-uniform shear stress distribution along the cross section. For rectangular cross sections this coefficient is given a value of $5/6$. From Eq. (5.1) it becomes evident that the reduction in natural frequency becomes more prominent with higher modes due to the presence of the n value.

The increase in displacement will also decrease the modal stiffness of the system. This diminished stiffness can be calculated by following Eq. (5.3) which uses the new reduced frequency.

$$K'_n = M_n(\omega'_n)^2 = \frac{mL}{2}(\omega'_n)^2 \tag{5.3}$$

The analytical solution may now be calculated using Eq. (4.2) from the previous section but with reduced values for the stiffness and natural frequencies to calculate the modal response parameters.

5.3 Results

The accuracy of the model will depend on how many elements the beam contains. With fewer number of elements, the response of the system will resemble more the response of the simply supported beam without considering shear deformation.

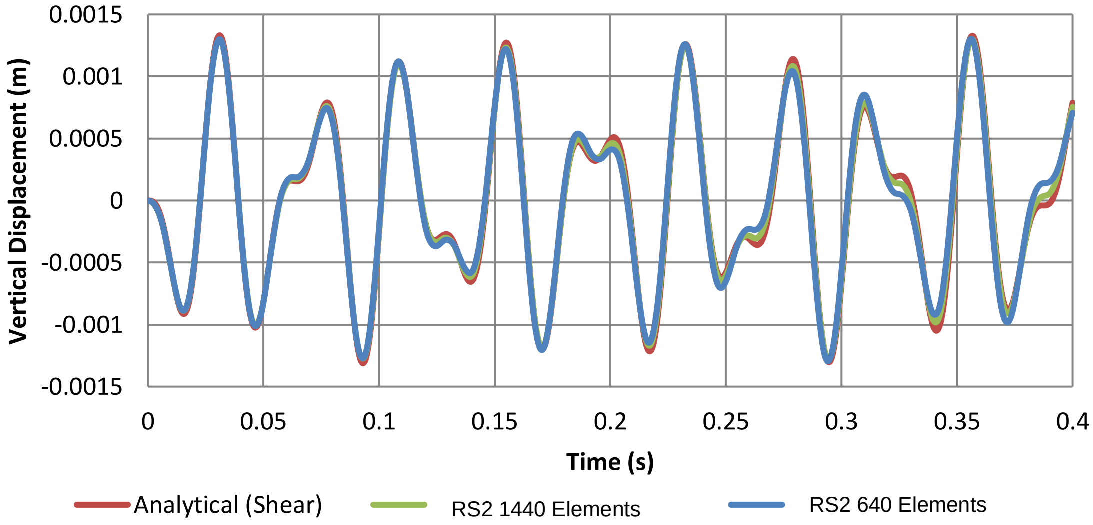

Figure 5-2: Vertical Displacement Response of the Midspan of the Beam

The results of two analyses is presented in Figure 5-2 that considered 640 and 1440 finite elements. The model with a greater number of elements exhibited a displacement response similar to that of the analytical solution that considered shear deformations. The coarser model was unable to capture that phenomenon as predicted.

The results demonstrate RS2's ability to capture complex material behavior during dynamic analysis provided that a sufficient number of elements have been used in the model.

5.4 References

Chopra, A. K. (1995). *Dynamics of Structures*. New Jersey: Prentice Hall.

5.5 Data Files

The input data files **Dynamic #005.fez, Dynamic #005_640.fez,** and **Dynamic #005_1440.fez** can be downloaded from the RS2 Online Help page for Verification Manuals.

6 Cantilever Beam Under Harmonic Load

6.1 Problem Description

This problem demonstrates behavior of a cantilever beam under harmonic load.

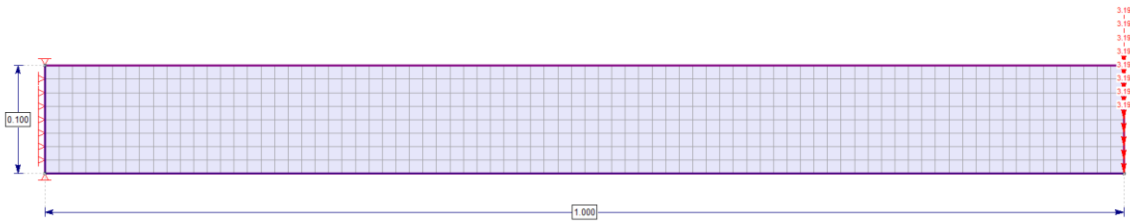

Figure 6-1: Cantilever beam modeled in RS2

Harmonic load is as below:

$$P(t)=3.1941\sin(\pi t/2) \quad \text{if} \quad 0<t\leq 2$$
$$P(t)=0 \quad \text{if} \quad t>2 \tag{6.1}$$

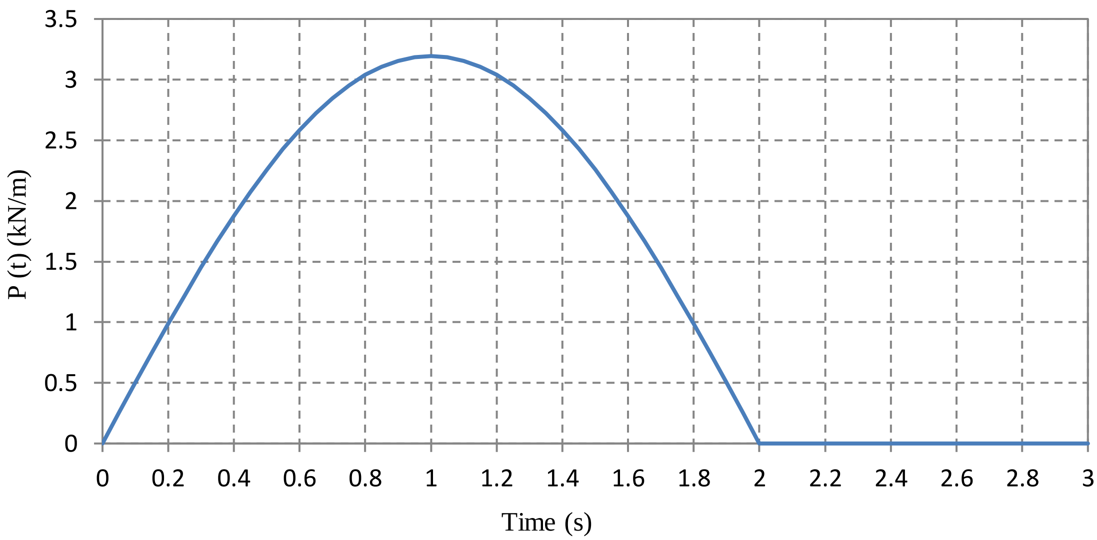

Figure 6-2: Harmonic load acting on the beam

Table 6.1: Model parameters

Parameter	***Value***
Material type	Elastic
Young's modulus (E)	38329.2 kPa
Poisson's ratio (v)	0.3
Unit weight (γ)	9.81 kN/m^3

Parameter	*Value*
Length (L)	1.0 m
Thickness (h)	0.1 m

6.2 Results

The beam displacement obtained using RS2 is compared with the solution obtained using MIDAS GTS. It can be seen that the two numerical tools provide a good agreement.

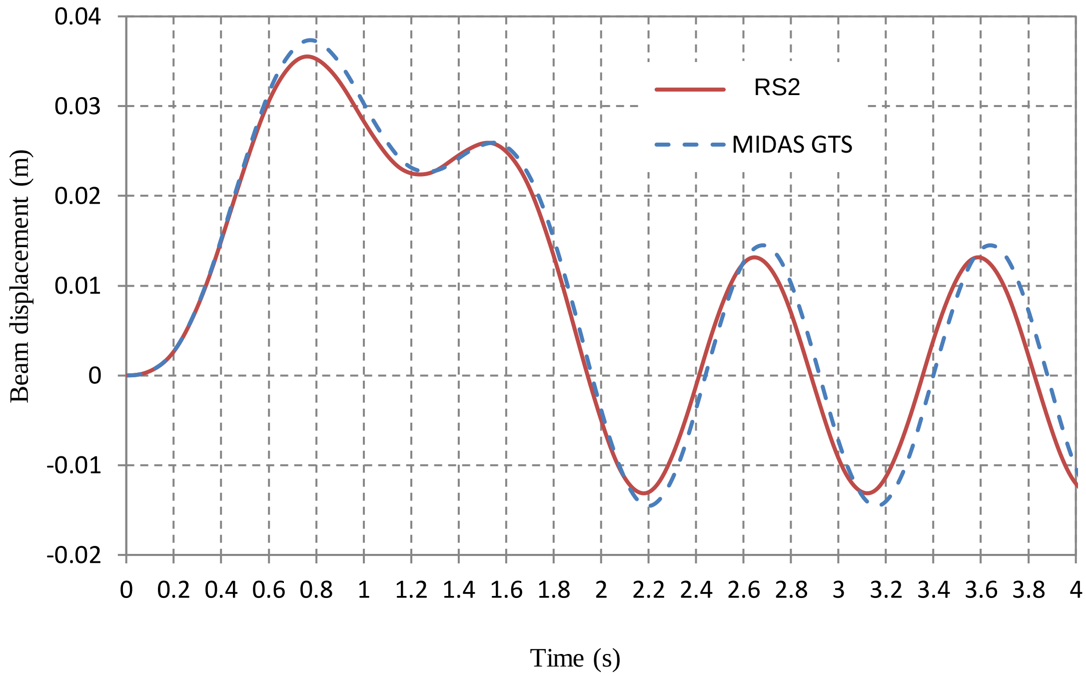

Figure 6-3: Midspan Displacement Response

6.3 References

J. M. Duncan and C. Y. Chang (1970), “Nonlinear analysis of stress and strain in soils”, J. of Soil Mech. and Foundation Division, ASCE, 96 (SM5), pp. 1629-1653.

6.4 Data Files

The input data file **Dynamic #006.fez** can be downloaded from the RS2 Online Help page for Verification Manuals.

7 Cantilever Beam Subjected to a Constant Point Load

7.1 Problem Description

This problem demonstrates behavior of a cantilever beam under a constant load. The properties of the cantilever are identical to the previous section's problem statement except that the Poisson's ratio here is zero, and that the beam is subjected to a constant load of 0.319 kN. Loading the cantilever with a constant load the fundamental period may be ascertained from the deflection response and compared to the theoretical first mode period. The mode shapes of the cantilever beam are not simple and described using hyperbolic cosine functions which does not allow for a concise analytical response function to be generated.

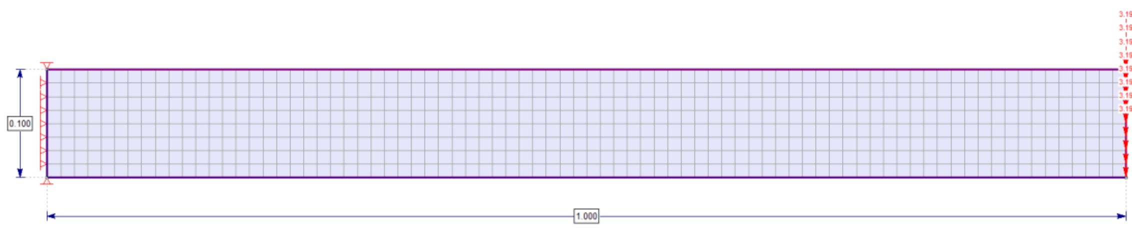

Figure 7-1: Cantilever beam modeled in RS2

Table 7.1: Model parameters

Parameter	***Value***
Material type	Elastic
Young's modulus (*E*)	38329.2 kPa
Poisson's ratio (*v*)	0
Unit weight (γ)	9.81 kN/m^3
Length (L)	1.0 m
Thickness (*h*)	0.1 m

7.2 Analytical Solution

The stiffness of a cantilever beam will be needed to determine the static stiffness of the system and it is presented below in Eq. (7.1).

$$K = \frac{3EI}{L^3} \tag{7.1}$$

The stiffness for this problem was determined to be 9.582 kN/m/m. Dividing the amplitude of the load by this stiffness produces a value of 0.0333 m for the static stiffness.

The first natural period of a cantilever is defined by Eq. (7.2). Evaluation that expression a fundamental period of 1.000 s was determined for this cantilever system.

$$\omega_i = \frac{3.516}{L^2}\sqrt{\frac{EI}{m}} \tag{7.2}$$

The analytical solution is going to idealize the system as a single degree of freedom system and the higher mode response of the cantilever is ignored. This is an imprecise idealization, but it will allow one to evaluate the general shape of the cantilever response. The response of a single degree of freedom system to a constant load is described below in Eq. (7.3).

$$u(t) = u_{static}[1 - \cos(\omega t)] \tag{7.3}$$

The maximum amplitude of the displacement will be twice that of the static displacement.

7.3 Results

The beam displacement obtained using RS2 is compared with the idealized response of a cantilever containing only response from the first mode.

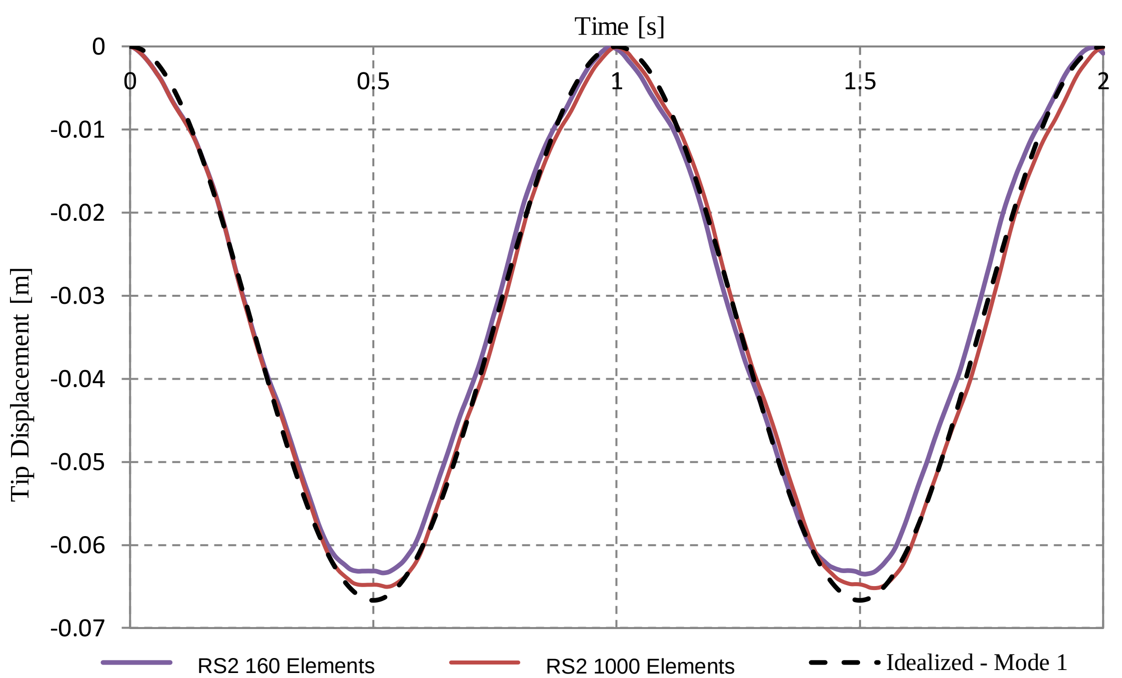

Figure 7-2: Cantilever Free End Vertical Displacement Response

Two models with differing number of elements were created and simulated to model the stated problem. The purpose of this was to determine the extent using larger element sizes alters the total model response. It is apparent from Figure 7-2 that two RS2 models visibly differ in amplitude and slightly in response period, with the model with a finer mesh exhibiting a period closer to the calculated fundamental period.

Though the two responses display discrepancies with the idealized response, especially a reduction in amplitude, the difference is likely due to the influence of higher mode responses. The deviation from a smooth sin curve is likely due to destructive interference of the higher modes. The response nevertheless exhibits a predominant period of 1s as predicted analytically and revealing the influence of the fundamental period on the total response.

7.4 References

Chopra, A. K. (1995). *Dynamics of Structures*. New Jersey: Prentice Hall.

7.5 Data Files

The input data file **Dynamic #007.fez** can be downloaded from the RS2 Online Help page for Verification Manuals.

8 Single Element with Spring and Damping

8.1 Problem Description

This section attempts to validate the spring and dashpot elements as well as the mass-proportional damping that is presently implemented in the dynamic module of RS2. In order to create a verifiable model, the problem had to be reduced to one that could be readily determined analytically, and for this reason the problem described here within is that of a single degree of freedom system.

The model consists of a single quadrilateral element with near rigid stiffness that provides mass to the dynamic system. The element is restrained in the horizontal direction and is only supported vertically by springs that provide the system's effective stiffness. The element's rigidity is supposed to refrain it from deforming and allow the springs to solely combat the imposed loads. The configuration of the system is presented below in Figure 8-1.

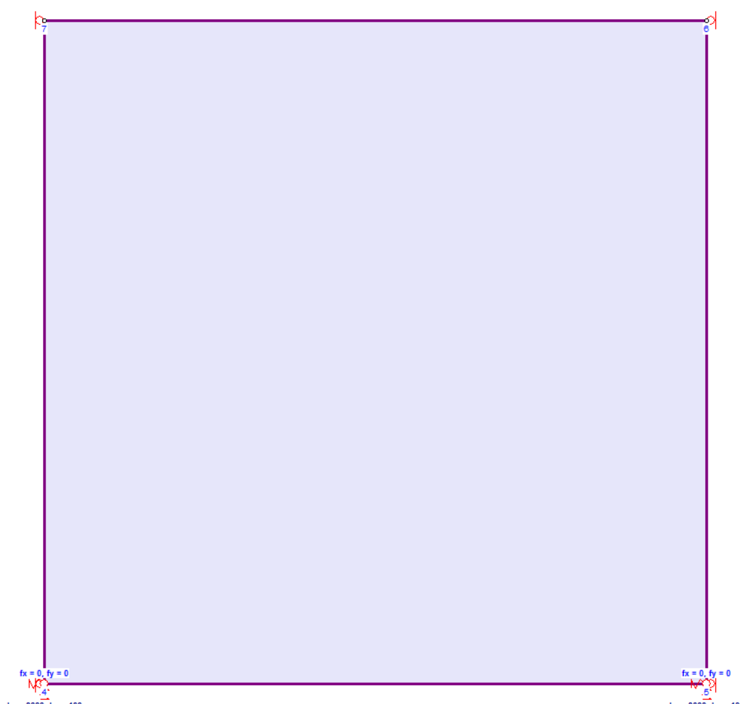

Figure 8-1: RS2 Model of the Problem Statement System

Table 8.1: Model Parameters

Parameter	***Value***
Material type	Elastic
Spring Stiffness (K)	100 kN/m/m
Unit weight (γ)	9.81 kN/m^3
Width & Height	0.5 m

The bottom nodes of the element where the springs are attached will both be subjected to an identical harmonic force with an amplitude of 10 kN and a frequency of 10 Hz or 62.8 rad/s. Therefore, the effective stiffness of the system is 200 kN/m/m and the amplitude of the total load is 20 kN.

The system will be modeled without damping, with damping provided by dashpot dampers and with damping provided by mass-proportioned Rayleigh damping. For this problem the damping level that is to be obtained is that of 10% of critical damping.

8.2 Damping Parameters

The coefficient of damper that is given to the dashpot damper is merely a fraction of the critical damping of the system and it is determined using Eq. (8.1).

$$C = \xi \times 2\sqrt{MK} \tag{8.1}$$

The mass of the system is 0.25 tons and the stiffness has been provided. Using these values 10% for the damping ratio, the damping coefficient was determined to be 1.414 kNs/m/m.

To ensure that the mass-proportional Rayleigh damping provided equivalent damping, the damping parameter was determined by simply dividing the damping coefficient by the value of the mass. This results in a Rayleigh damping parameter of 5.657.

8.3 Analytical Solution

Since the system is effectively a single degree of freedom system the analytical solutions are readily available. The natural frequency was determined to be 28.28 rad/s by using Equation (8.2).

$$\omega_n = \sqrt{\frac{K}{M}} \tag{8.2}$$

For an undamped single degree of freedom system with no initial displacement or velocity the displacement response function is defined by Equation (8.3). The first sinusoidal function represents the particular solution which oscillates at the forcing frequency whereas the second sinusoidal function is the complimentary solution that oscillates at the natural frequency. Typically, in a damped system the complimentary solution is the transient response of the system that dissipates over time, however in an undamped system it is ever present

$$u(t) = \frac{Po}{K} R \sin(\overline{\omega} t - \theta) - \frac{\beta}{1-\beta^2} \sin \omega_n t \tag{8.3}$$

Where β is the ratio between the forcing and natural frequencies, R_d is the amplitude reduction factor of the particular solution and θ is the phase angle. These variables are defined below.

$$\beta = {}^{\bar{\omega}}/_{\omega_n}$$

$$R = \frac{\beta}{|1-\beta^2|}$$

$$\theta = \begin{cases} 0, & \beta < 0 \\ \pi, & \beta > 0 \end{cases}$$

For this system β was found to be 2.221, the reduction factor R had a value of 0.254 and the phase angle had the value of π.

A damped system possesses a similar response function except that the particular solution decays exponentially and there is some period elongation due to the damping. The steady-state solution retains the same form, but the reduction factor and phase angle definitions are modified to account for damping in the system. The damped response function of this system with no initial velocity or displacement is presented in Eq. (8.4).

$$u(t) = \frac{P_0}{K} R_d \sin(\bar{\omega}t - \theta_d) + e^{-\xi\omega t}[A\cos(\omega_d t) + B\sin(\omega_d t)] \tag{8.4}$$

Where the variables A and B are determined based on the initial conditions of the system. For a system that is initially stationary, the variables are defined below.

$$A = -\frac{P_0}{K} R_d \sin(-\theta_d)$$

$$B = \frac{\xi\omega A - \frac{P_0}{K} R_d \bar{\omega} \cos(-\theta_d)}{\omega_d}$$

The new damped parameters are defined below.

$$R_d = \frac{1}{\sqrt{(1-\beta^2)^2 + (2\xi\beta)^2}}$$

$$\theta_d = \tan^{-1}\left(\frac{2\xi\beta}{1-\beta^2}\right)$$

$$\omega_d = \omega_n\sqrt{1-\xi^2}$$

For the damped problem the reduction factor R_d has a value of 0.254, the phase angle is -0.1124 rad and the damped natural frequency is 28.14 rad/s. The initial condition variables A and B were determined to be -0.002851 and -0.05667 respectively.

8.4 Results

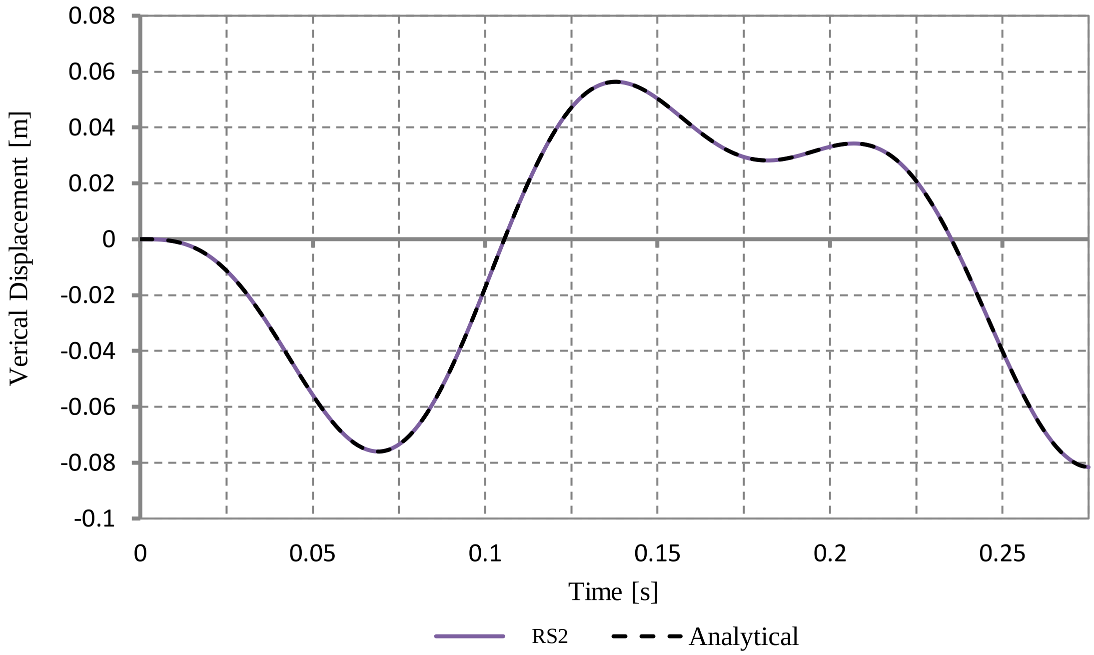

Figure 8-2: Undamped Displacement Response

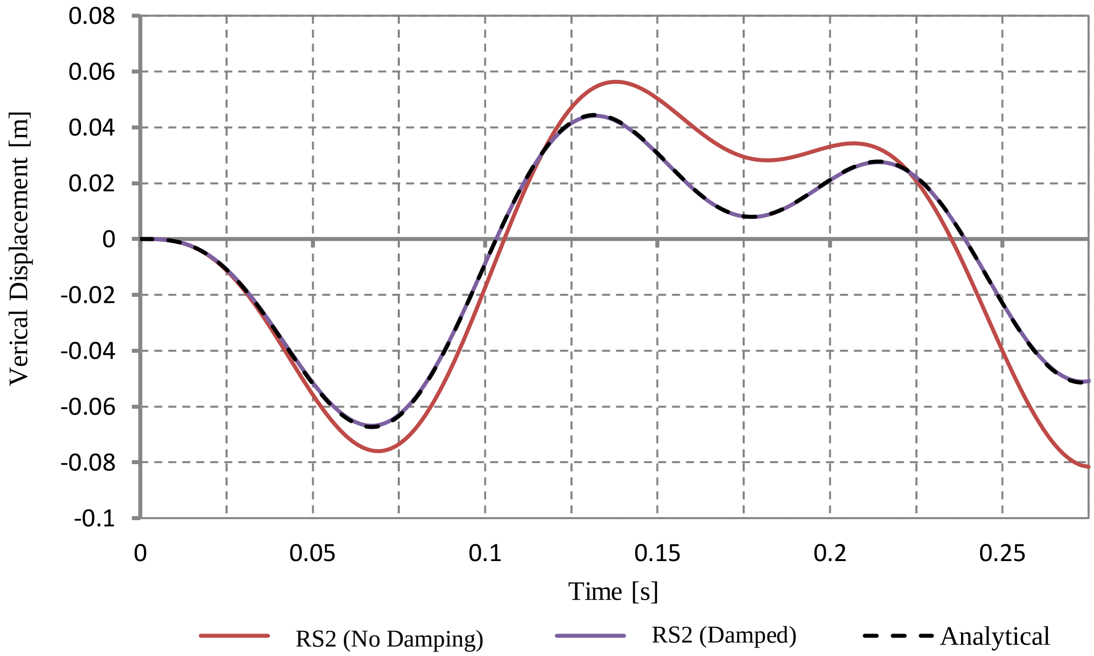

Figure 8-3: Damped Displacement Response using Dashpot Dampers

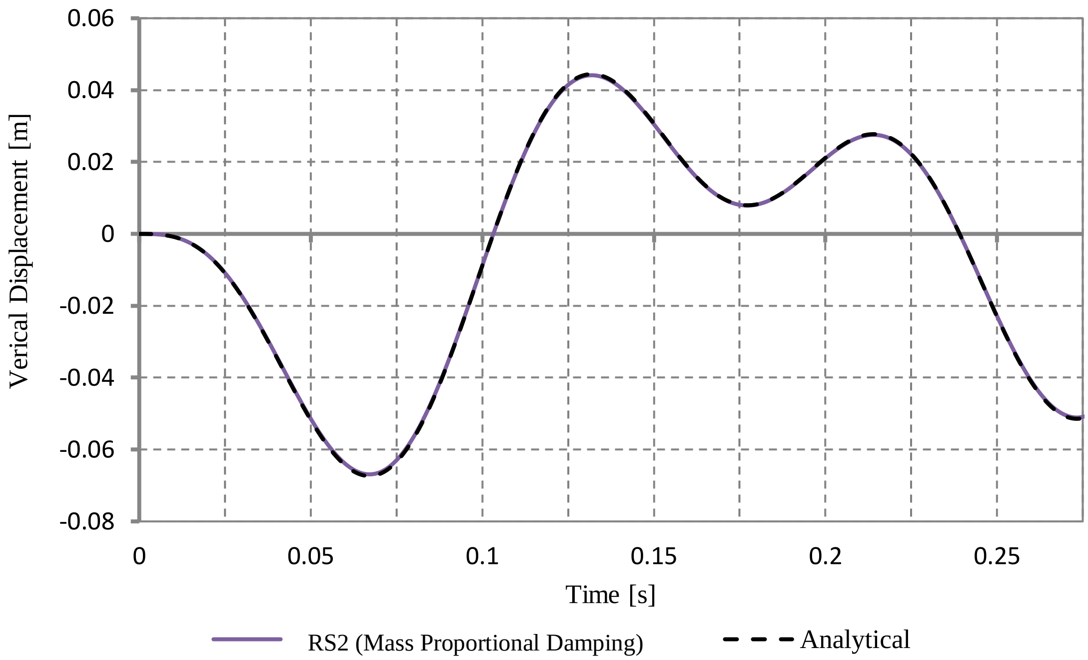

Figure 8-4: Damped Displacement Response using Mass Proportional Damping

The response of the both the damped and undamped models presented in Figure 8-2 and Figure 8-3 show great agreement with the analytical solution. This demonstrates that the springs and dashpot dampers have been implemented correctly in RS2.

The results of the RS2 model using mass proportional damping rather than dashpot dampers is presented in Figure 8-4.The results of this model was similarly in agreement with the analytical solution, demonstrating that the mass proportional Rayleigh damping has been effectively implemented.

8.5 Data Files

The input data files **Dynamic #008.fez, Dynamic #008_Damped.fez,** and **Dynamic #008_NoDamped.fez** can be downloaded from the RS2 Online Help page for Verification Manuals.

9 Two Element Model with Imposed Motion

9.1 Problem Description

This section attempts to validate the RS2 functionality that allows users to impose displacement, velocities and accelerations rather than an external force. These functions are important for users to be able to apply the seismic loads effectively.

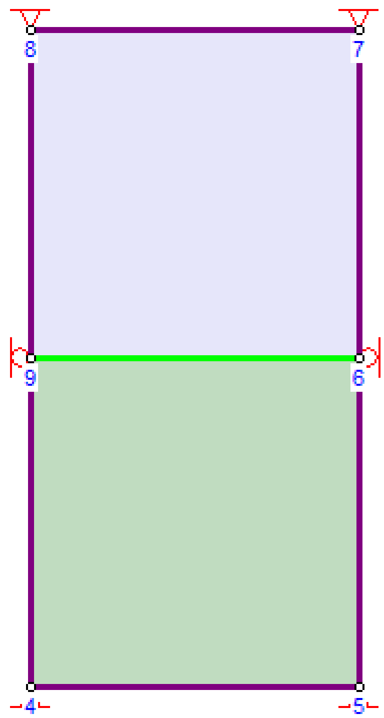

Figure 9-1: RS2 model of the problem statement system

The model, as depicted in Figure 9-1, consists of two quadrilateral elements with a shared an edge that is free to move vertically and all other nodes being restrained. One element is massless and contributes all of the stiffness to the system. The other element possesses negligible stiffness and contributes the mass to the system. The properties of the system are defined below.

Table 9.1: Model Parameters

Parameter	***Value***
Stiff Element	
Material type	Elastic
Young’s modulus (E)	20 000 kPa
Unit weight (γ)	0.01 kN/m^3
Poisson’s ratio (v)	0
Width & Height	0.5 m

Parameter	*Value*
Mass Bearing Element	
Material type	Elastic
Young's modulus (E)	1 kPa
Unit weight (γ)	27 kN/m^3
Poisson's ratio (v)	0
Width & Height	0.5 m

The model will be subjected to a half-period sine load of a total 10 kN amplitude acting on the free edge that the two elements share. The load will be delayed by 0.05s from the start of the simulation. The load that node 6 and 9 is subjected to is displayed in Figure 9-2.

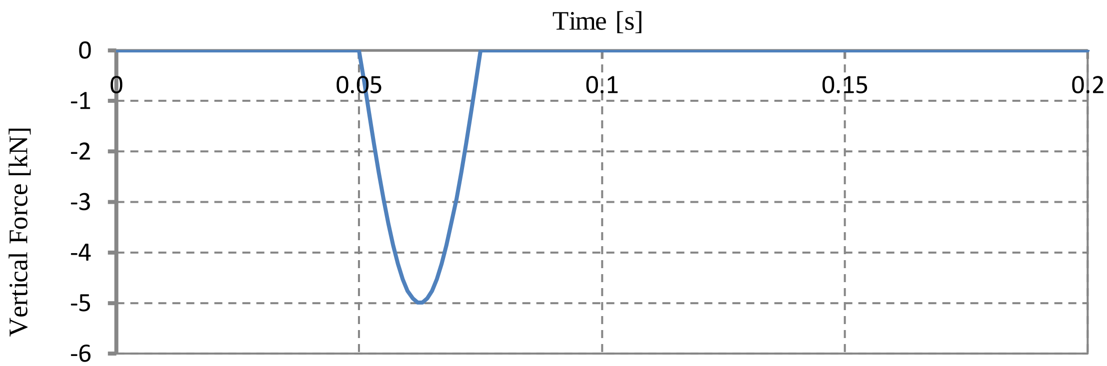

Figure 9-2: Half Sine Nodal External Force

The response of system to this external force will be compared to that to a model that has an equivalent acceleration history applied at the boundaries. The imposed acceleration required is determined by dividing the external force function by the mass of the system. This vertical acceleration will then be applied at nodes 7 and 8 which will be allowed to move vertical. The displacement response from the previous model will be compared to the displacement of the edge shared by the elements relative to the now moving boundary. If these two results are equal, then the acceleration history has been properly implemented.

$$a(t) = \begin{cases} 0 & t < 0.5 \\ \frac{1}{m}\sin[\overline{\omega}(t - 0.05)] & 0.5 \leq t < 0.55 \\ 0 & t \geq 0.55 \end{cases} \quad (9.1)$$

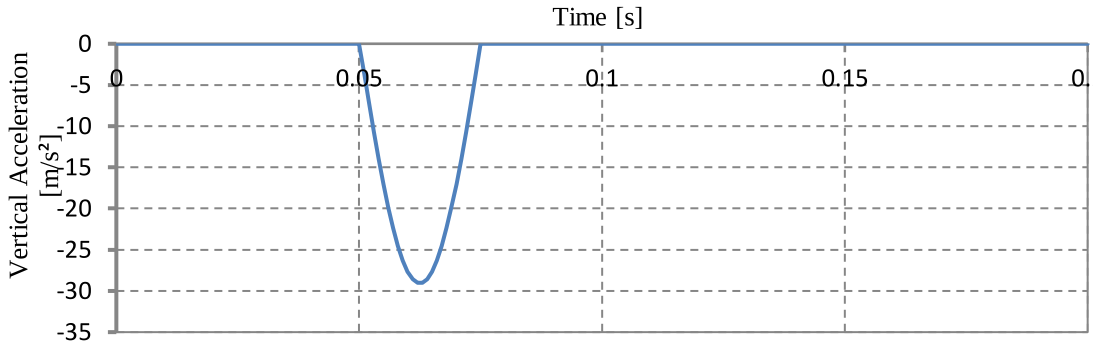

Figure 9-3: Half Sine Nodal Acceleration at the Boundary

9.2 Analytical Solution

The exact solution for the system's response to the sinusoidal load may be calculated using Duhamel's integral or another analysis tool however it is not necessary for this validation example. Different loading approaches are being evaluated and provided both produce the same response function, then it shows that they have been adequately implemented.

The reason that two loading conditions must produce the same response is because of the differential equation that is being solved by the integration scheme. For a single degree of freedom system, the spring force is calculated from a relative displacement whereas the inertial force is dependent on the absolute or total acceleration of the node as presented in Equation (9.2).

$$m\ddot{u}_{total} + ku_{relative} = 0 \quad (9.2)$$

Decomposing the acceleration into the contribution of the ground and the relative acceleration a new equation of motion may be determined that is presented in Eq. (9.2). This equation of motion represents the system that is being analyzed in the external force loading case. Eq. (9.2b) represents the system with acceleration imposed on the boundary which has been shown to be an identical system.

$$m(\ddot{u}_g + \ddot{u}_{relative}) + ku_{relative} = 0 \quad (9.2b)$$

$$m\ddot{u}_{relative} + ku_{relative} = -m\ddot{u}_g = F(t) \quad (9.3)$$

The mass of the system in the system is only provided by the mass bearing element at two free nodes. Given the weight and size of the element the mass at each node able to move vertically is 0.172 tons. The stiffness the stiff element provides to each node is 10000 kN/m/m. Given the expression for natural frequency in Eq. (9.4) the system's natural frequency is 241.1 rad/s corresponding to a fundamental period of 0.02606 s.

$$\omega_n = \sqrt{\frac{K}{M}} \quad (9.4)$$

In order to impose a velocity or displacement on the boundary, the integral and double integral of the acceleration must be calculated to determine the boundary velocity and acceleration. The results of the integration are presented below in Eq. (9.5) and (9.6) and they will be used in the displacement and velocity-imposed segment of the analysis.

$$v(t) = \begin{cases} 0 & t < 0.5 \\ -\frac{1}{m\bar{\omega}}\cos[\bar{\omega}(t-0.5)] + \frac{1}{m\bar{\omega}} & 0.5 \le t < 0.55 \\ \frac{2}{m\bar{\omega}} & t \ge 0.55 \end{cases} \tag{9.5}$$

$$u(t) = \begin{cases} 0 & t < 0.5 \\ -\frac{1}{m\bar{\omega}^2}\sin[\bar{\omega}(t-0.5)] + \frac{(t-0.5)}{m\bar{\omega}} & 0.5 \le t < 0.55 \\ \frac{2(t-0.55)}{m\bar{\omega}} + \frac{0.05}{m\bar{\omega}} & t \ge 0.55 \end{cases} \tag{9.6}$$

9.3 Results

The response of the model system with a fixed top boundary and force applied at the center nodes is presented in Figure 9-4. The response is being compared to that of a similar system with an equivalent acceleration applied at the boundary. The two responses are identical which confirms that the imposed acceleration function has been implemented correctly.

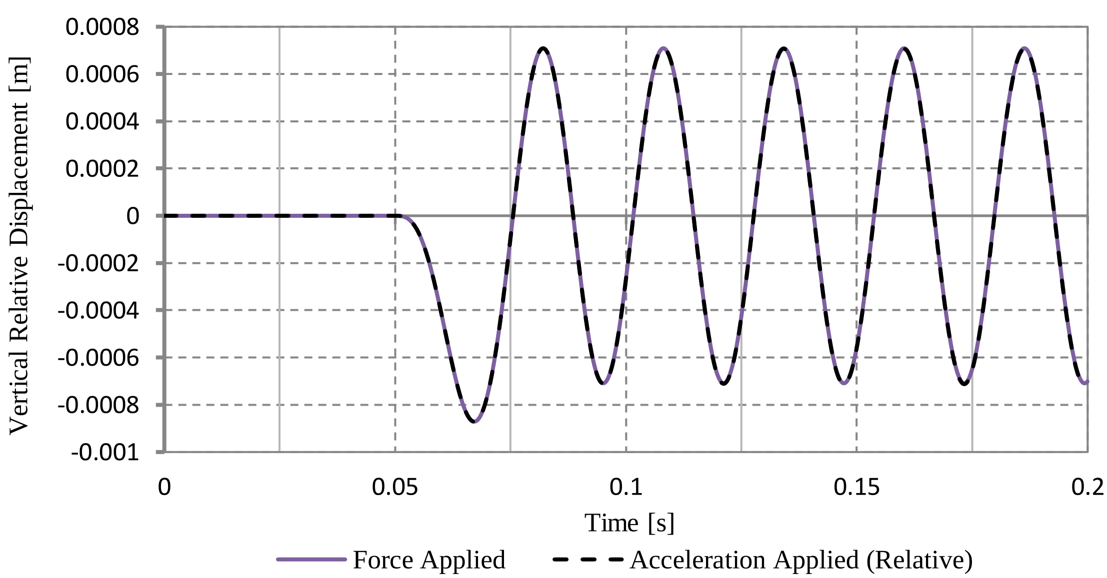

Figure 9-4: Vertical Displacement of the Center Nodes

An equivalent may be analyzed if the displacement that had been calculated previous and presented in Eq. (9.6) is imposed on the boundary rather than the acceleration. The absolute displacement of the boundary node is presented below in Figure **9-5** and is shown to be identical to that of the displacement produced from the model with imposed acceleration.

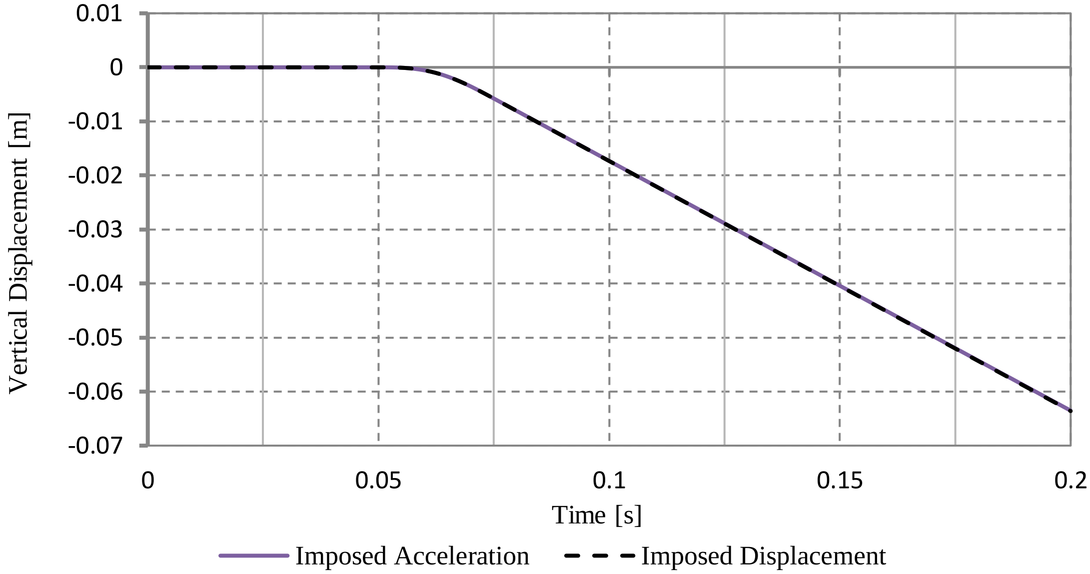

Figure 9-5: Absolute Displacement of the Support Node

Figure 9-6 demonstrates that the displacement response of the center nodes due to imposing displacement is identical to that of imposed acceleration loading which was shown to reproduce the force loading example. The three system's identical response demonstrates that the imposing displacement and acceleration functions are implemented correctly in RS2.

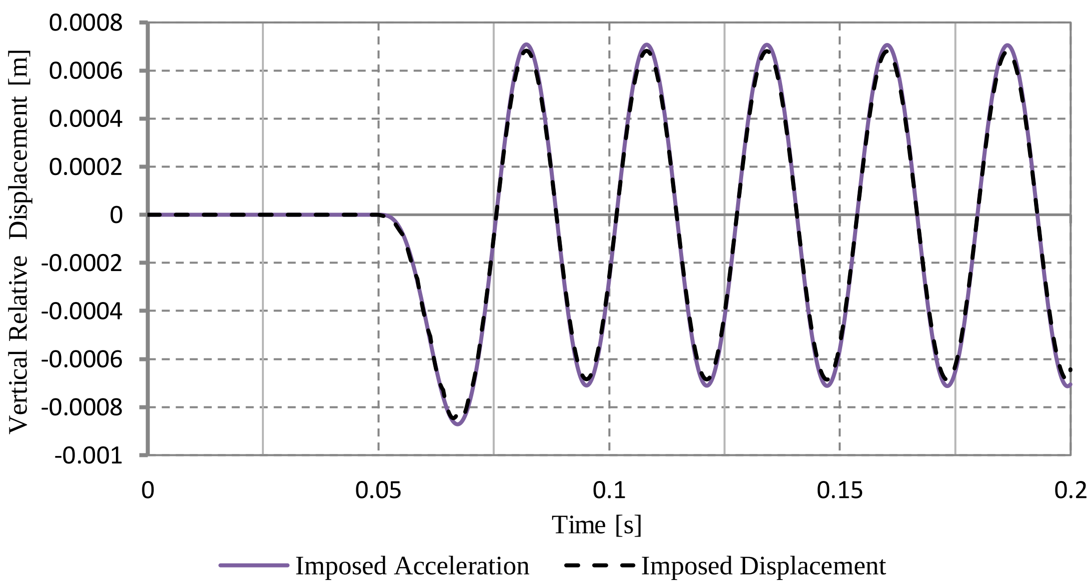

Figure 9-6: Relative Displacement of the Center Nodes

9.4 Data Files

The input data files **Dynamic #009-1.fez** and **Dynamic #009-2.fez** can be downloaded from the RS2 Online Help page for Verification Manuals.

10 One-Dimensional S-Wave Propagation

10.1 Problem Description

This problem addresses S-wave propagation in a one-dimensional soil column. The model is allowed to move only in the horizontal direction. A prescribed horizontal displacement of 0.01m is applied to the bottom of the column. In order to test viscous dashpot, the dashpots are applied to the top of the soil column to replace the fixed boundary. The geometry of the problem is shown in Figure 10-1. The material properties used in the model are summarized in Table 10.1.

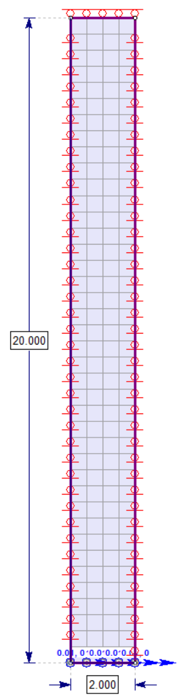

Figure 10-1: RS2 model of a soil column

Table 10.1: Model parameters

Parameter	***Value***
Material type	Elastic
Young's modulus (E)	20000 MPa
Poisson's ratio (v)	0.25

10.2 Analytical Solution

Velocity of S-wave in the column is:

$$\beta = \sqrt{\frac{G}{\rho}} \tag{10.1}$$

Where, G is the shear modulus:

$$G = \frac{E}{2(1+\upsilon)} \tag{10.2}$$

In this problem, the analytical S-wave velocity is 62.64 m/s.

The time necessary for a middle point to start moving is:

$$t = \frac{L/2}{\beta} = 0.16s \tag{10.3}$$

The shear wave is induced by moving the bottom edge of the mode by 0.01 m and maintaining that imposed displacement for the entirety of the simulation. For the fixed top boundary case it is expected that the shear wave will reflect from the fixed boundary and repeatedly influence the midspan horizontal deflection. The viscous boundary should absorb the incoming shear wave and eliminate any reflection waves.

10.3 Results

Displacements of a point at the middle of the column are analyzed in two cases: no damping and with dashpots applied to the top of the column. The results are shown in Figure 10-2 and Figure 10-3. It can be seen that the middle point starts to move just before at 0.16s which agrees well with the analytical solution. The displacement at the point is dropped to zero at a 0.48s when the S-wave comes back due to lack of viscous boundaries. If viscous dashpots are used, a constant displacement of 0.01 m is observed after 0.16s. Results of a similar problem calculated from Plaxis are given in Figure 10-4 and Figure 10-5 for reference.

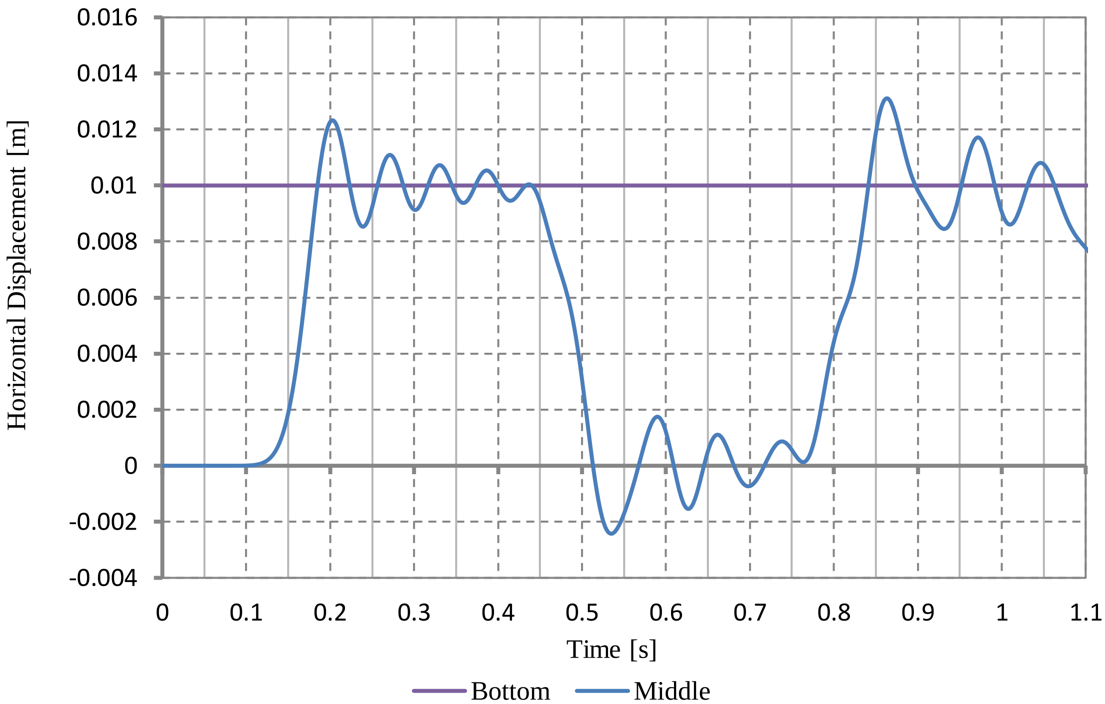

Figure 10-2: Displacement at the middle of the soil column-undamped fixed boundary

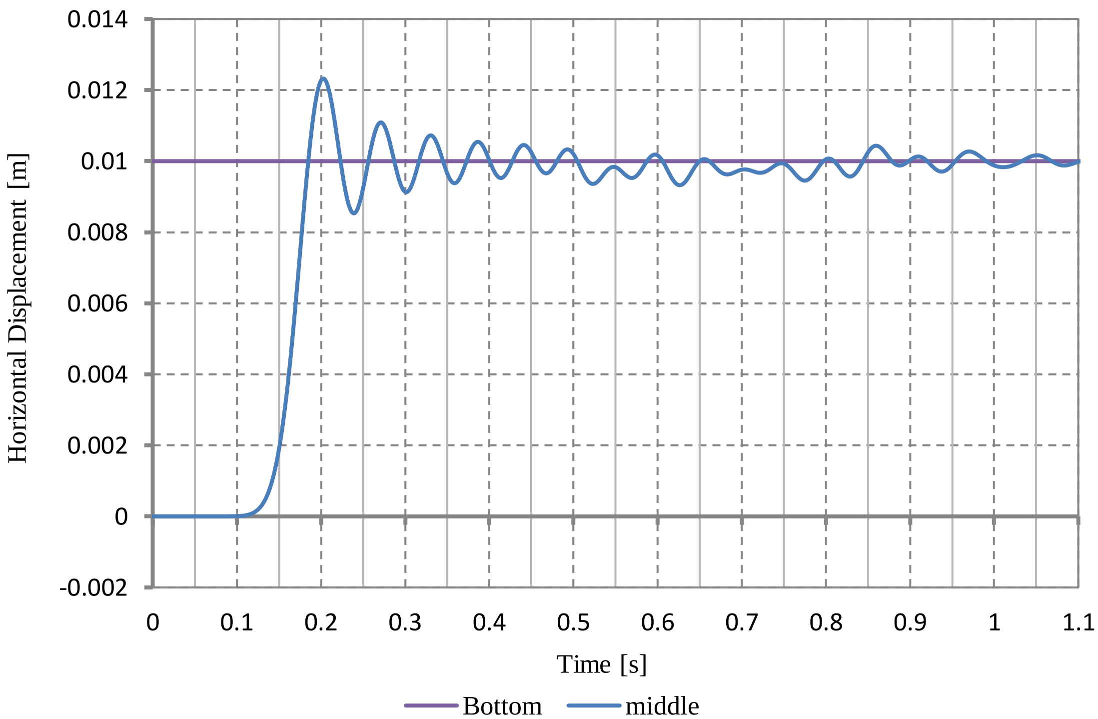

Figure 10-3: Displacement at the middle of the soil column-viscous boundary

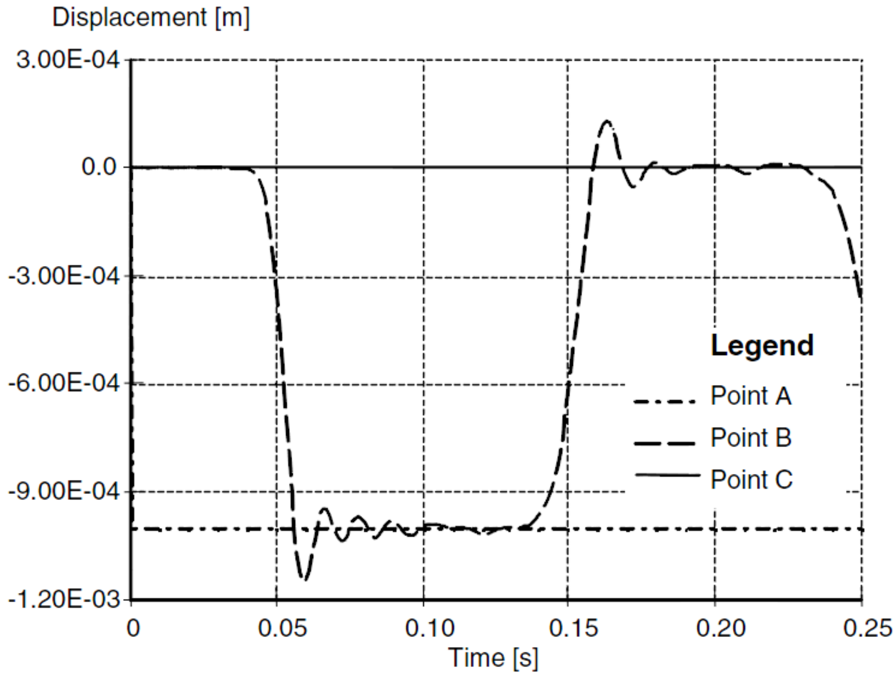

Figure 10-4: Displacements-undamped (from Plaxis)

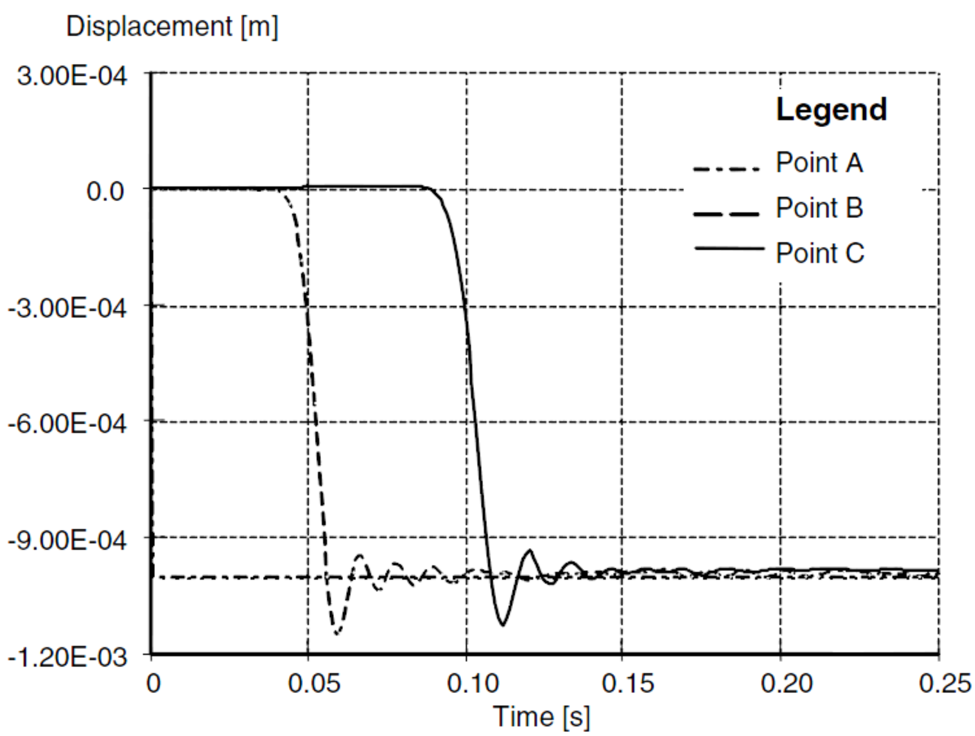

Figure 10-5: Displacements-viscous boundary (from Plaxis)

10.4 References

Brinkgreve, R. B. (2002) Plaxis 2D Version 8.4: Reference, Scientific and Dynamic Manuals, Lisse, Balkema.

10.5 Data Files

The input data files **Dynamic #010-1.fez** and **Dynamic #010-2.fez** can be downloaded from the RS2 Online Help page for Verification Manuals.

11 Lamb's Problem: S-Wave and P-Wave Propagation

11.1 Problem Description

This problem addresses Lamb's problem [1] which is wave propagation in a semi-infinite elastic medium subjected to an impulsive force applied at the surface. In RS2, the field problem is simulated using a symmetric model extending to 100 m in the horizontal direction and 30 m in the vertical direction. Viscous boundaries are introduced at the bottom of the model as well as the maximum horizontal boundaries. The geometry of the problem is shown in Figure 11-1. The point load acting on the top left of the model is approximated by a triangle load with the duration of 0.025 and the load started after 0.05s. The magnitude of the load is 50kN. The value of 7.957747 kN (50kN/2π) was used in the model because only 1 rad was model. The material properties used in the model are summarized in Table 11.1. No artificial damping was used in the simulation.

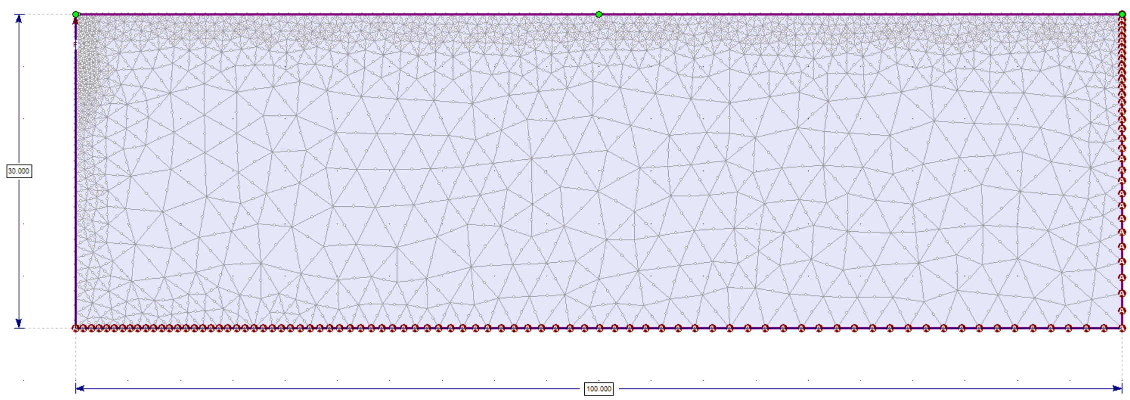

Figure 11-1: RS2 model of the problem

Table 11.1: Model parameters

Parameter	*Value*
Material type	Elastic
Young's modulus (E)	50000 MPa
Poisson's ratio (v)	0.25
Unit weight (γ)	20 kN/m^3

11.2 Results

Time-vertical displacement at relationship a point on the surface, 50 m away from the source as calculated by RS2 is shown in Figure 11-2. Results of a similar problem calculated from Plaxis are given in for reference. Please note that artifical damping values were employed in Plaxis to obtain the results.

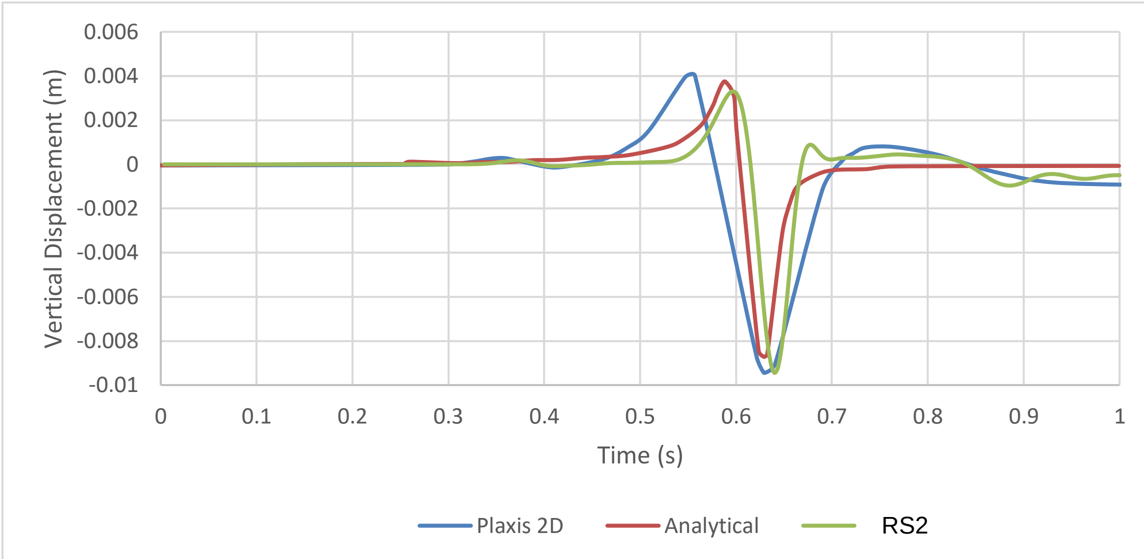

Figure 11-2: Vertical Displacement at x = 50m

11.3 References

Brinkgreve, R. B. (2012) Plaxis 2D Dynamic Module – Version 2011: Verification, Scientific and Dynamic Manuals, Lisse, Balkema.

11.4 Data Files

The input data file **Dynamic #011.fez** can be downloaded from the RS2 Online Help page for Verification Manuals.

12 Hysteretic Damping

12.1 Introduction

The equivalent-linear method is commonly used to determine the wave propagation for material subjected to cyclic loading. For example, when soil and rock are subjected to seismic motions, the material behaviour involves a modulus reduction curve. The equivalent-linear method accounts for the material nonlinearity indirectly by employing a modulus degradation. In order to allow the users to reproduce the modulus reduction response calculated using the equivalent-linear method, a material model is developed to directly account for the strain-dependent modulus and damping function in RS2.

In this model, we focus on the hysteretic material response under repetitive loading-unloading cycles. As shown in the loading-unloading plot in Figure 12-1, the initial loading is interrupted by a complete unloading, then followed by a loading that continues up to the maximum magnitude of the initial loading, then repeat. This case verifies the capability of the RS2 model on capturing the effect of nonlinearity of elastic material.

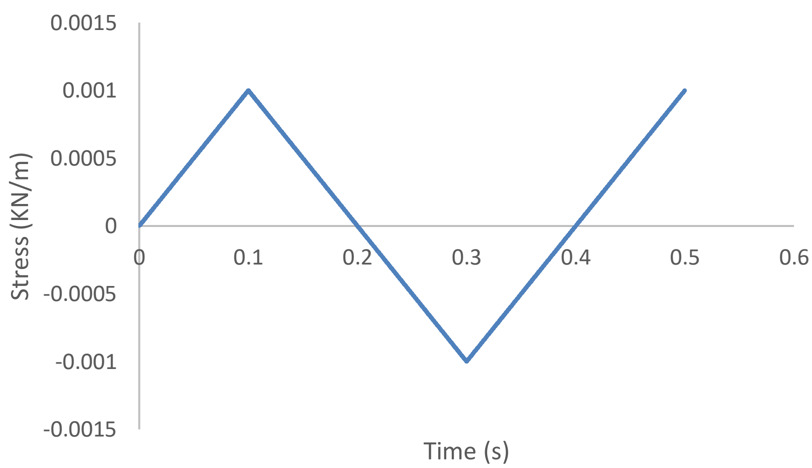

Figure 12-1: Loading-Unloading Cycle

A model as shown in Figure 12-2 is used to assess the hysteretic damping response of the Mohr-Coulomb material model in RS2. Two cyclic loadings are applied at the top and middle of a simple square model, respectively. The amplitude of the loading applied in the middle of model is half of the loading applied at the top (Figure 12-2). Figure 12-1 shows the loading applied at the top of the model.

The non-linear model in RS2 is developed based on the following:

$$E_{max} = E_0(\frac{bp+a}{p_{ref}+a})^m \tag{1.9}$$

$$E = E_{max}(1 + \alpha \frac{\gamma}{\gamma_y})^r \tag{1.10}$$

Where E is the elastic modulus,
γ is the deviatoric strain depends on the loading history,
p_{ref} is the reference pressure,
p is the mean pressure,
m is usually between 0.5 and 1.0,
r is the degradation parameter which should be less than zero,
and a, b and α are material parameters.

When an increment of strain is applied to the material, each principal direction is checked for a possible change in the loading direction. Once the direction of loading is changed the stiffness regains a maximum recoverable value in the order of its initial value, E_{max}.

12.2 Geometry and Properties

The material properties and dynamic analysis parameters are shown in Table 12.1 and Table 12.2. Parameter m in this case is equal to zero because the maximum young's modulus (E_{max}) is constant.

Table 12.1 – Material Properties

Analysis	ϕ′ (deg.)	E (kPa)	γ (kN/m³)	υ	a	b	m	Pref	alpha	gamma y	r
Martin et al.	35	2.57e08	1000	0.286	0	1	0.0	100	1	0.00011	-0.475

Table 12.2 – Rayleigh Damping Parameters

α	β
1.5	0.002

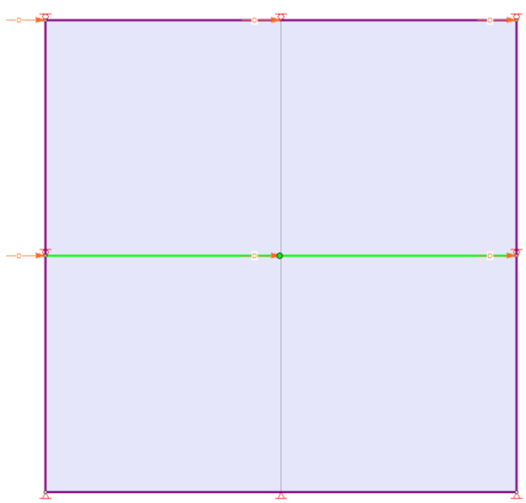

Figure 12-2: RS2 Model Geometry

12.3 Results

Figure 12-3 illustrates that the RS2 hysteretic response curve agrees with the response from FLAC default model. The x-axis contains the shear strain, while the y-axis represents the effective shear stress. Two curves are almost identical. The stress-strain path in Figure 12-3 demonstrates that the stress and strain increase as the initial loading increases, then decreases during the unloading part, followed by another increase during the reloading. Since it is an elastic model, the strain path always follows the same loop.

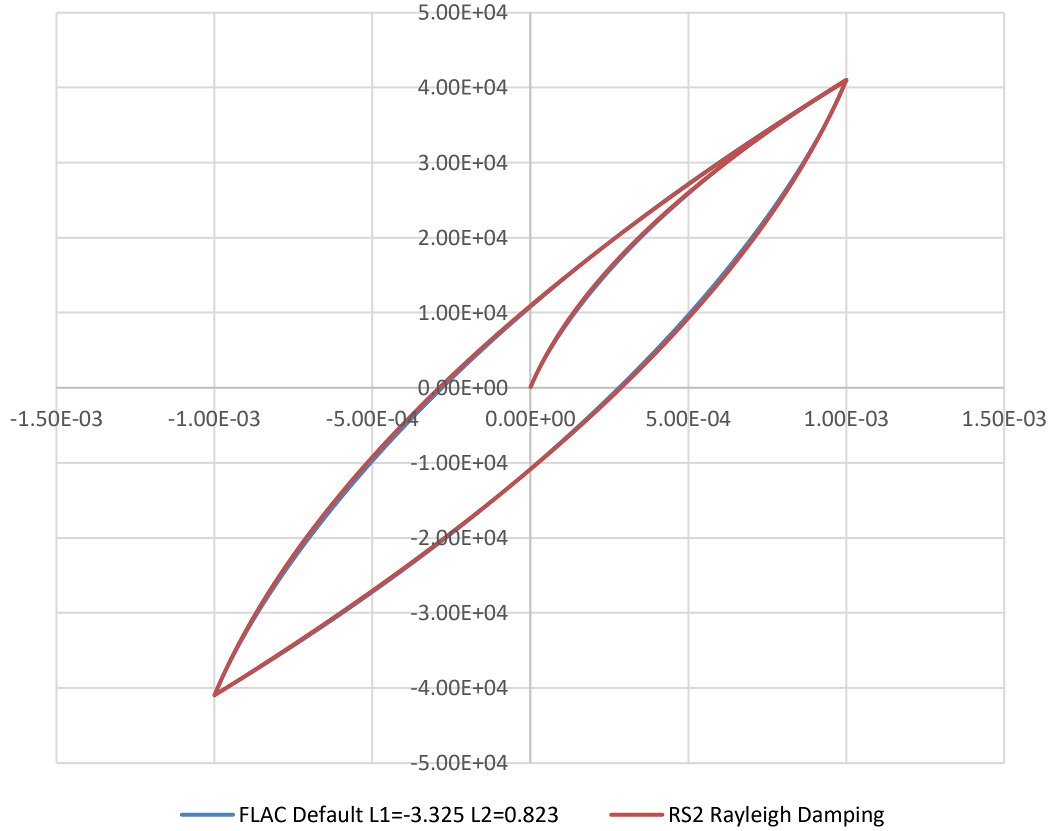

Figure 12-3: Hysteretic Damping Graph

12.4 References

Itasca Consulting Group Inc. (2011). *FLAC version 7.0: Dynamic Analysis*.

12.5 Data Files

The input data file **Dynamic #012.fez** can be downloaded from the RS2 Online Help page for Verification Manuals.

13 Harmonic Shear Wave

13.1 Introduction

This verification is from FLAC example 1.7.4 Slip Induced by Harmonic Shear Wave:

Itasca Consulting Group Inc. (2011). FLAC Dynamic Analysis Version 7.0 (pp. 1.252 – 1.261).

This case focuses on the energy dissipation given a homogeneous media under a shear wave, separated by a discontinuity in the middle. Absorb boundary is assigned to the top and bottom boundary of the model acting as non-reflective boundary, vertical restraints are assigned to the two lateral boundaries. The material model is elastic.

13.2 Problem Description

A joint boundary is used to simulate the discontinuity in the middle of the media, four joint boundary cohesions are assigned to four model to simulate the non-slip surface (2.5MPa) and slip surface (0.02MPa, 0.1MPa and 0.5MPa). The friction angle of the joint boundaries is equal to zero.

A shear wave in terms of frequency w and time t is given as $\sin(wt)$ and applied in the horizontal direction at the bottom boundary of the models. Please note that the magnitude of the shear wave needs to be doubled in this case, taking consideration of two non-reflective boundary.

The RS2 response of the four models are used to determine the coefficient of transmission (T), reflection (R) and absorption (A). The coefficients are then compared with the analytical solution derived by Miller 1978 where the coefficients are given as following:

$$R = \sqrt{\frac{E_R}{E_I}} \tag{1.1}$$

$$T = \sqrt{\frac{E_T}{E_I}} \tag{1.2}$$

$$A = \sqrt{1 - R^2 - T^2} \tag{1.3}$$

Where E_R , E_I, E_T are calculated following:

$$E = \rho \, c \int_{t_1}^{t_1+T} v_s^2 dt \tag{1.4}$$

Where ρ is the material density, c is the velocity of the propagating shear wave and v_s is the particle velocity in the x direction. For E_R , the energy flux is calculated by determining the difference in velocities at the top and bottom points. While for E_I and E_T the energy flux is determined by using the velocities at the bottom point and the top point, respectively.

In order to determine the coefficients T, R and A, the interest of this case is the x-displacement and x=velocity at the top and bottom time queries as indicated in Figure 13-2.

13.3 Geometry and Properties

Table 13.1: Material Properties

E (kPa)	γ (kN/m³)	υ
2.5e+07	26.5	0.25

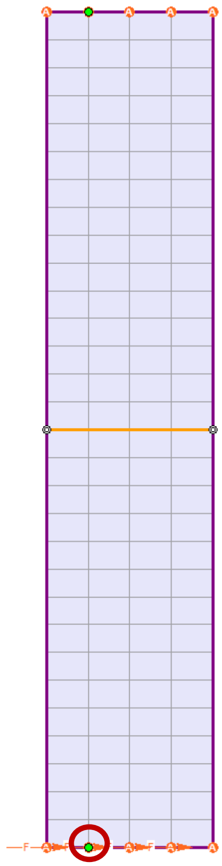

Figure 13-1: RS2 Model Geometry

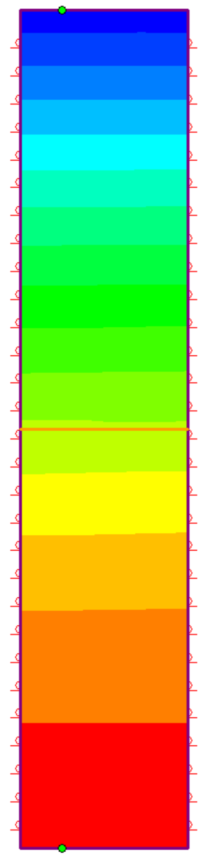

Figure 13-2: Example Horizontal

13.4 Results

Figure **13-3** compares the coefficients determined from RS2 results with the analytical solution by Miller (1978) in terms of the dimensionless parameter:

$$\frac{w\gamma U}{\tau_s}$$

Where τ_s is the cohesion of discontinuity, U is the displacement amplitude for the bottom point in the case of a non-slip surface, γ equals to the square root of density and shear modulus and w is the frequency of the applied wave, which is equal to 1 Hz in this case.

It can be seen from Figure **13-3** that the coefficients from RS2 results agree well with the analytical solution by Miller (1978).

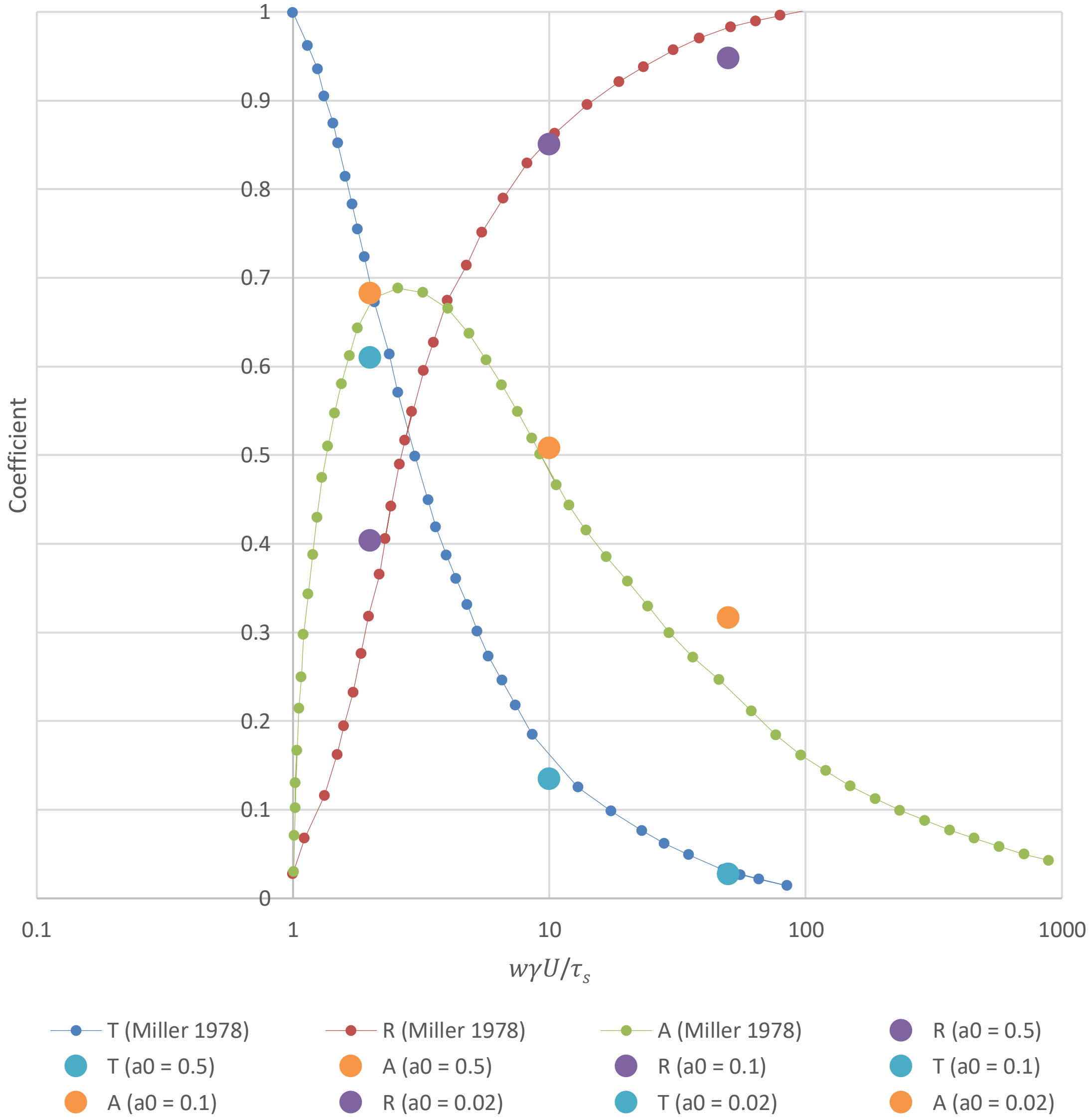

Figure 13-3: Comparison of the coefficients calculated from RS2 output with the analytical solution from Miller 1978

13.5 Data Files

The input data files under the folder **Dynamic #013** can be downloaded from the RS2 Online Help page for Verification Manuals.

14 Internal Blast

14.1 Introduction

This verification is from FLAC example 1.7.5 Hollow Sphere Subject to an Internal Blast:

Itasca Consulting Group Inc. (2011). FLAC Dynamic Analysis Version 7.0 (pp. 1.262 – 1.271).

This case demonstrates the propagation of a wave caused by a spherical internal pressure in a sphere and a rectangle. *Absorb* boundary is assigned to the outer boundary of the model, either circular or rectangular the simulate the isotropic and infinite medium that the sphere and rectangle are embedded in. *Axisymmetric* and *plane strain* are chosen as the analysis type for the circular and rectangular models respectively, given the nature of these two geometries. The material model in this problem is elastic.

14.2 Problem Description

The dynamic response of the two models is simulated in RS2. A pressure equals to 1kPa is applied at the spherical inner boundaries of both models. Figure 14-1 indicates the model geometry in RS2. The interest of this case is the propagation of the responsive wave translated by plotting the horizontal displacement at different time queries located at different distances from the internal pressure. The results are compared to the analytical solution by Blake (1052), governed by an equation of compressional wave velocity C_p, time t, a potential function Ø and Laplacian operator V:

$$\frac{\partial^2 ø}{\partial t^2} = C_p^2 \text{V}^2 ø \tag{1.1}$$

In this case, the potential function used to find the radial displacement can be expressed as following:

$$u_r = -\frac{p_0 a^3 k}{\rho C_p^2 r^2}[-1 + \sqrt{2-2v}\exp(-a_0\tau)\cos\left(w_0\tau - tan^{-1}\frac{1}{\sqrt{4k-1}}\right) + \frac{p_0 a^3 k}{\rho C_p^2 r}[\frac{a_0}{C_p}\sqrt{2-2v}\exp(-a_0\tau)\cos\left(w_0\tau - tan^{-1}\frac{1}{\sqrt{4k-1}}\right) + \frac{w_0}{C_p}\sqrt{2-2v}\exp(-a_0\tau)\cos\left(w_0\tau - tan^{-1}\frac{1}{\sqrt{4k-1}}\right) \tag{1.2}$$

Where p_0 is the pressure applied on the model;
a = radius of the sphere;
$K = \frac{1-v}{2(1-2v)}$;
$v = Poisson's\ ratio$;
$r = radial\ coordinate$;

$a_0 = \frac{C_p}{2ak}$ = radiation damping constant;
$\tau = t - \frac{r-a}{C_p}$ and
$w_0 = \frac{c}{2aK}\sqrt{4K-1}$ = natural frequency.

14.3 Geometry and Properties

Table 14.1: Material Properties

E (kPa)	γ (kN/m^3)	υ
2.4975e+07	16.75	0.25

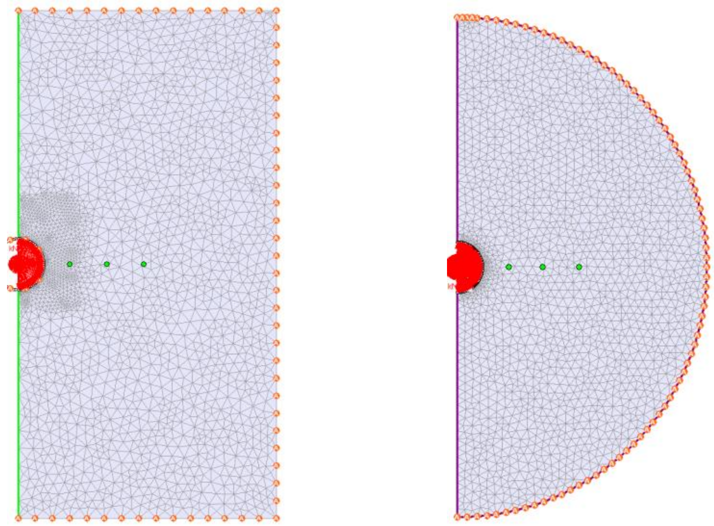

Figure 14-1: RS2 Model Geometry

14.4 Results

The response in Figure 14-2 and Figure **14-3** illustrates that farther locations transmit less wave. Figure **14-3** demonstrates that the resulted x-displacement from RS2 using circular and rectangular boundary is almost identical and both match the analytical solution derived by Blake (1952).

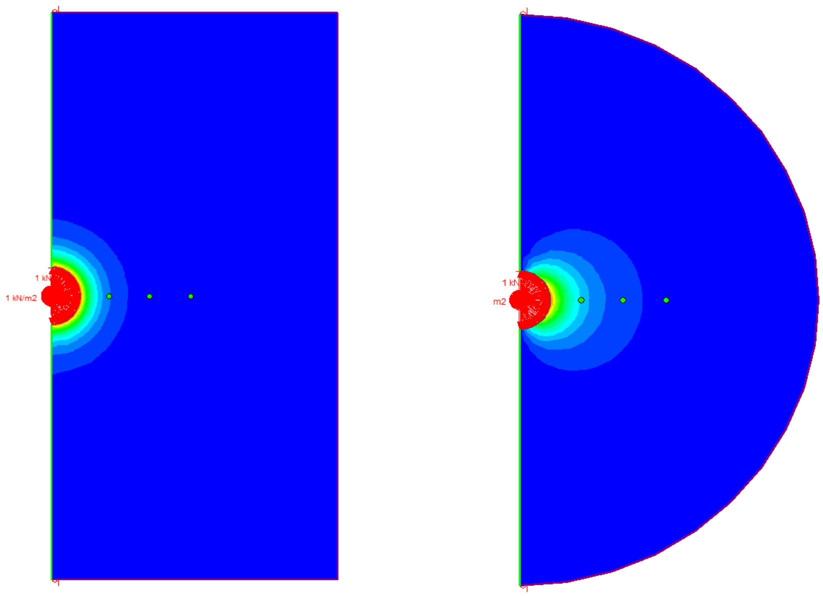

Figure 14-2. Example Horizontal Displacement Results in RS2

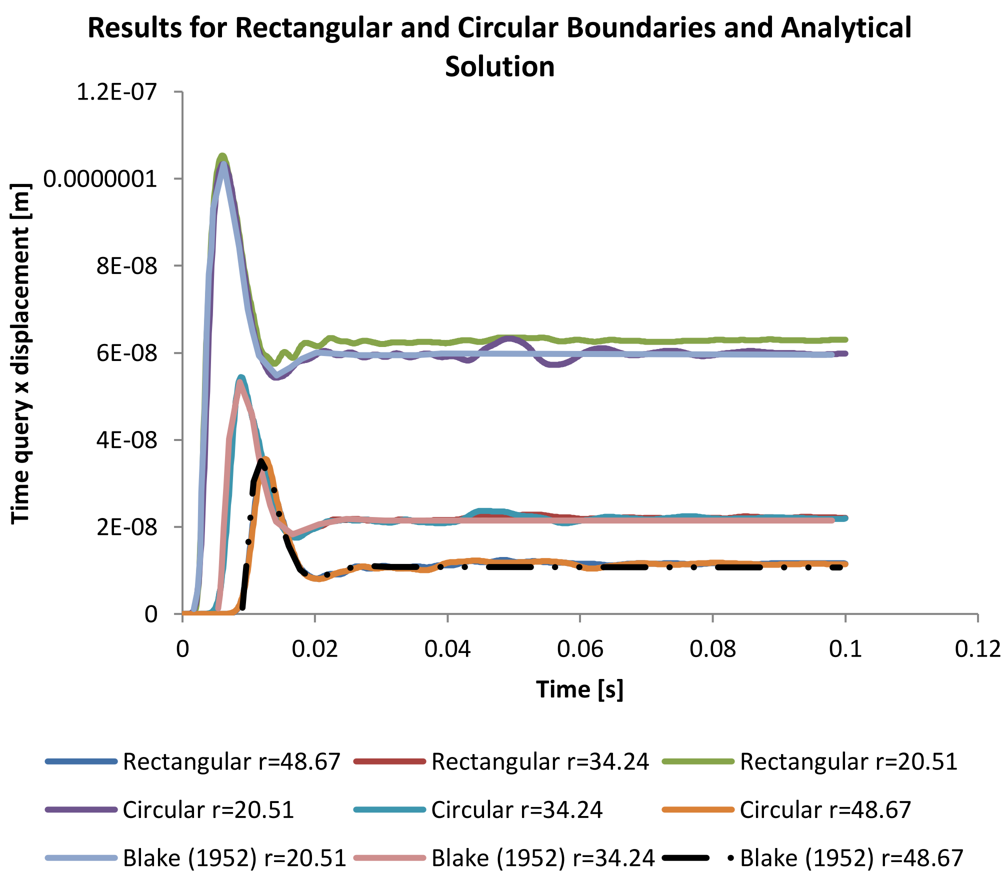

Figure 14-3: X-Displacement vs Time at Different Time Queries in Comparison with the Analytical Solution by Blake (1952)

14.5 References

Itasca Consulting Group Inc. (2011). *FLAC version 7.0: Dynamic Analysis*.

Blake, F.G. (1952). "Spherical Wave Propagation in Solid Media", J.Acous. Soc. Am., 24(2), 211-215.

14.6 Data Files

The input data files under the folder **Dynamic #014** can be downloaded from the RS2 Online Help page for Verification Manuals.

15 Machine Foundation

15.1 Introduction

This verification is from FLAC example 1.7.6 Vertical Vibration of a Machines Foundation:

Itasca Consulting Group Inc. (2011). FLAC Dynamic Analysis Version 7.0 (pp. 1.272 – 1.278).

This case concerns the vertical response of the soil directly underneath a rigid strip footing, under the cyclic loading applying on the footing. Half of the model is simulated taken advantage of the symmetry and therefore *fix in x-direction* is assigned to the left boundary. *Absorb* boundary is assigned to the right and bottom boundary of the model. Five different frequency ratio a_0 (0.5, 1, 1.5, 2, 2.5) is used in five models. The stiff footing is modelled as beam element with a very large young's modulus to result in uniform vertical response and limit the horizontal and rotational movement of the soil directly underneath the footing. The material model in this problem is elastic.

15.2 Problem Description

The dynamic response of the five models is simulated in RS2. The cyclic loading applied on the footing is in terms of a_0 and therefore different in five models.

The cyclic loading P is expressed as P = $P_0 \sin(wt)$, where P_0 is the force amplitude, w is the operational frequency and t is the run time for each model as shown in Table 15.2.

Figure 15-1 indicates the model geometry in RS2. A compliance function of operational frequency and phase angle is proposed by Gazetas and Roesset (1979). The interest of this case is the compliance function calculated from vertical displacement of the upper left corner in comparison with the theoretical one by Gazetas and Roesset (1979). The compliance function expresses the amplitude of motion δ_0 in terms of the machine force P_0 as following:

$$\delta_0 = \frac{\delta_0 G}{P_0}\left[\frac{f_{1,v}^2 + f_{2,v}^2}{(1-ba_0^2 f_{1,v}^2)^2 + (ba_0^2 f_{2,v}^2)^2}\right]^{1/2} \tag{1.1}$$

Where G is the shear modulus of material, $f_{v,1}$ represents the recoverable part of the deformation while $f_{v,2}$ represents the non-recoverable part.

The dimensionless mass b and frequency ratio a_0 are defined as:

$$b = \frac{M}{\rho B^2} \quad a_0 = \frac{wB}{V_s} \tag{1.2}$$

Where ρ = density, V_s = s-wave velocity of the soil, B = half-width of the strip foundation, which is 10ft in this case, M = total foundation mass per unit length and w is the operational frequency.

15.3 Geometry and Properties

Table 15.1: Material Properties

E (kPa)	γ (pcf)	υ
1.12e+07	128.8	0.4

Table 15.2: Dynamic Properties

a_0	W	β	α	Time (s)
0.5	50.00	0.001000	2.50	1.2566
1	100.00	0.000500	5.00	0.6283
1.5	150.00	0.000333	7.50	0.4189
2	200.00	0.000250	10.00	0.3142
2.5	250.00	0.000200	12.50	0.2513

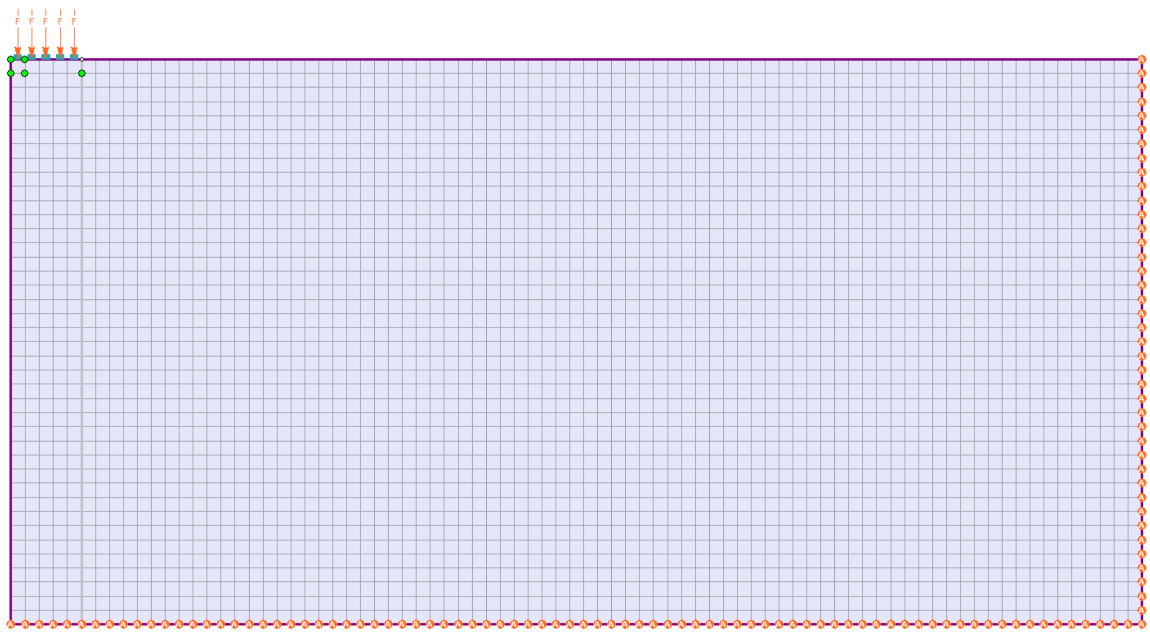

Figure 15-1: RS2 Model Geometry

15.4 Results

Figure 15-3 illustrates that the compliance function calculated from RS2 response compare with the theoretical values well. It should be noted that the agreement is better at higher a_0 because the boundary is supposed to be located at several wavelengths away, otherwise the Rayleigh waves do not damp as efficiently.

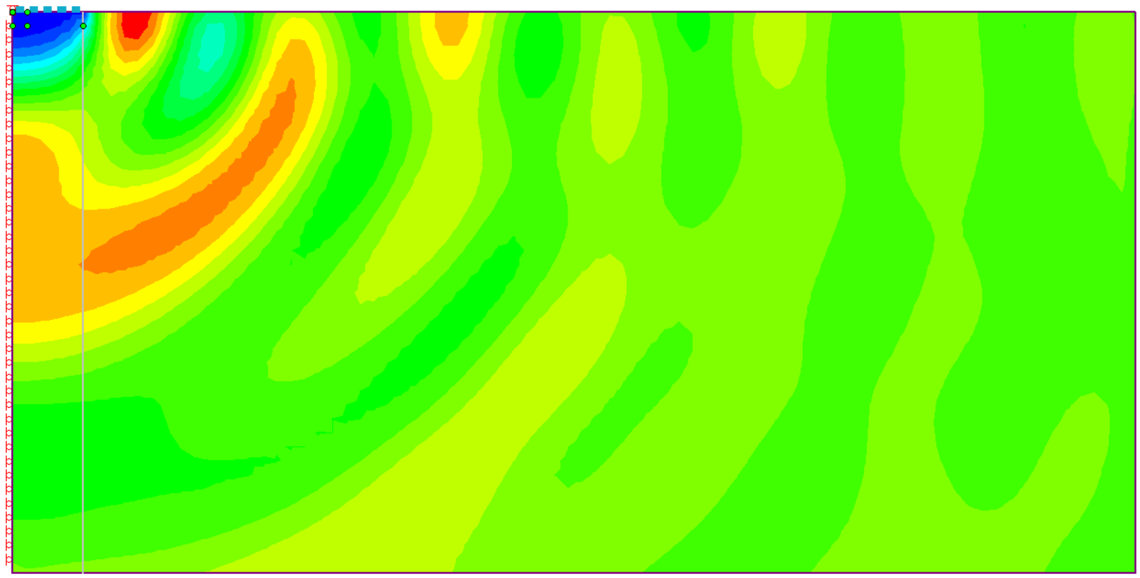

Figure 15-2: Example Vertical Displacement Results in RS2

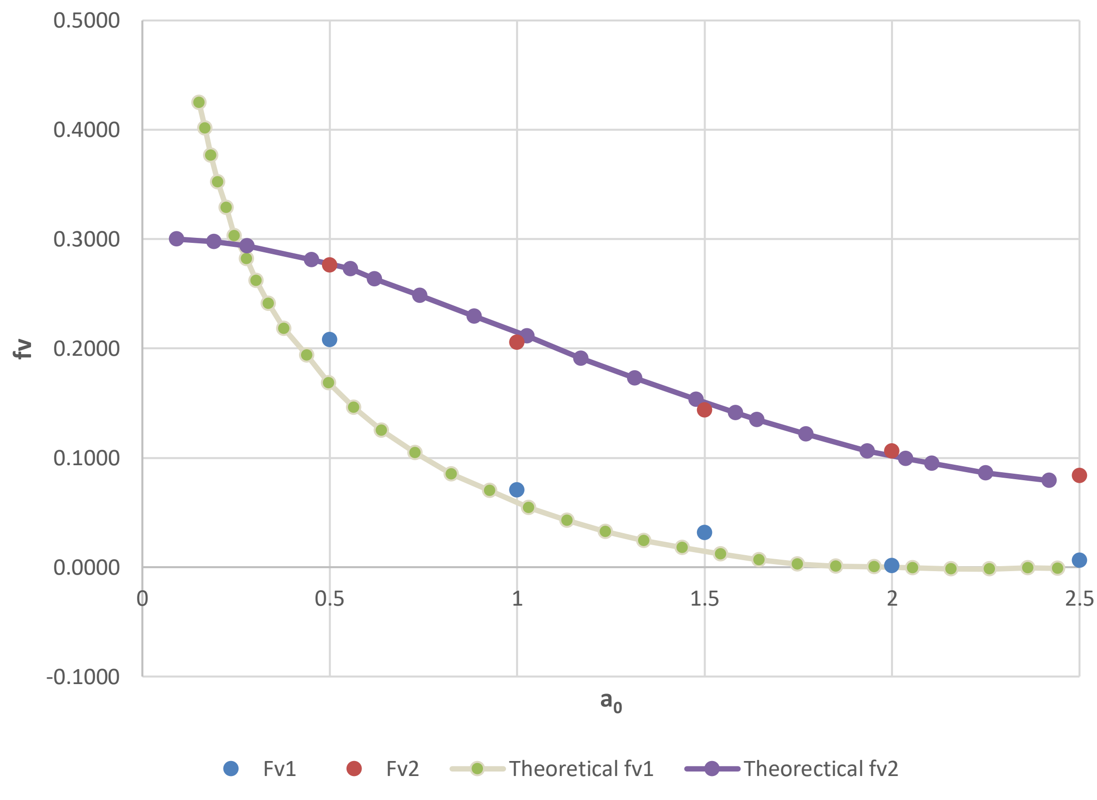

Figure 15-3: Compliance function comparison between calculated output from RS2 and theoretical values by Gazetas and Roesset (1979)

15.5 References

Itasca Consulting Group Inc. (2011). *FLAC version 7.0: Dynamic Analysis*.

Gazetas, G., and J. M. Roesset. (1979). *"Vertical Vibration of Machine Foundations"*, J, Geotech., Div. ASCE. 105(GT12), 1435-1454.

15.6 Data Files

The input data files under the folder **Dynamic #015** can be downloaded from the RS2 Online Help page for Verification Manuals.

16 Seismic Response Case

16.1 Introduction

This verification concerns the deconvolution analysis in RS2.

This model consists of a 300mm tall column, a dynamic velocity is applied at the base of the model. Two models with different dynamic boundary conditions are compared. During the initial stage, the boundary conditions are the same for both models, *fix in x-displacement* is assigned all around the model and *fully fixed* is assigned to the bottom. During the dynamic stage, two different boundary conditions (*transmit* and *tie*) are assigned all around the model in two models respectively and *absorb* is assigned to the bottom in both models. The models are run with two damping ratios of 3% and 5%. The material model in this problem is elastic.

16.2 Problem Description

The dynamic response of the two models is simulated in RS2. A compliant base with absorbing boundary is used at the base of both models. Figure 16-1 indicates the model geometry in RS2. The interest of this problem is the velocity and acceleration at the surface of the column under ground motion. An outcrop signal generated in DEEPSOIL with a damping ratio of 3% and 5% is inputted in RS2 at the base of the column, the output velocity and spectral acceleration at the top of the column are compared to the DEEPSOIL results.

16.3 Geometry and Properties

Table 16.1: Material Properties

E (kPa)	γ (kN/m^3)	υ
2.6e+07	24	0.4

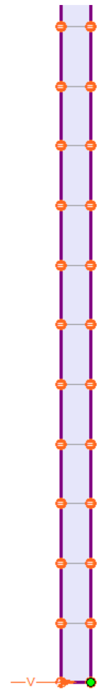

Figure 16-1: RS2 Model Geometry

16.4 Results

Figure 16-2 illustrates that the RS2 output ground motions compares well with the outcrop signal from DEEPSOIL either with a damping ratio of 5% or 3%. The insignificant difference between the two curves is due to the difference in material damping.

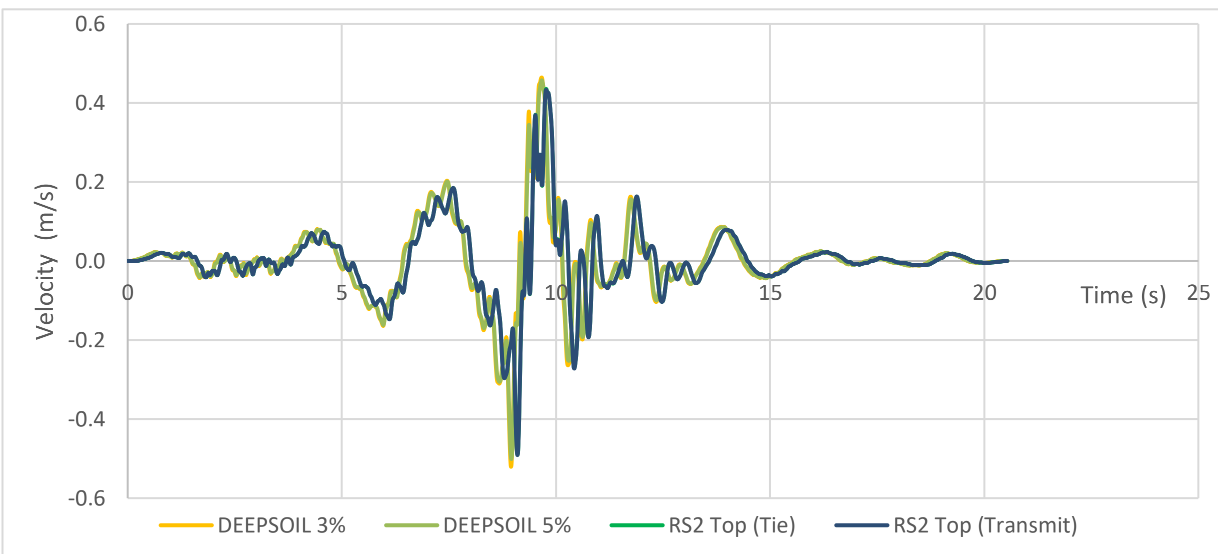

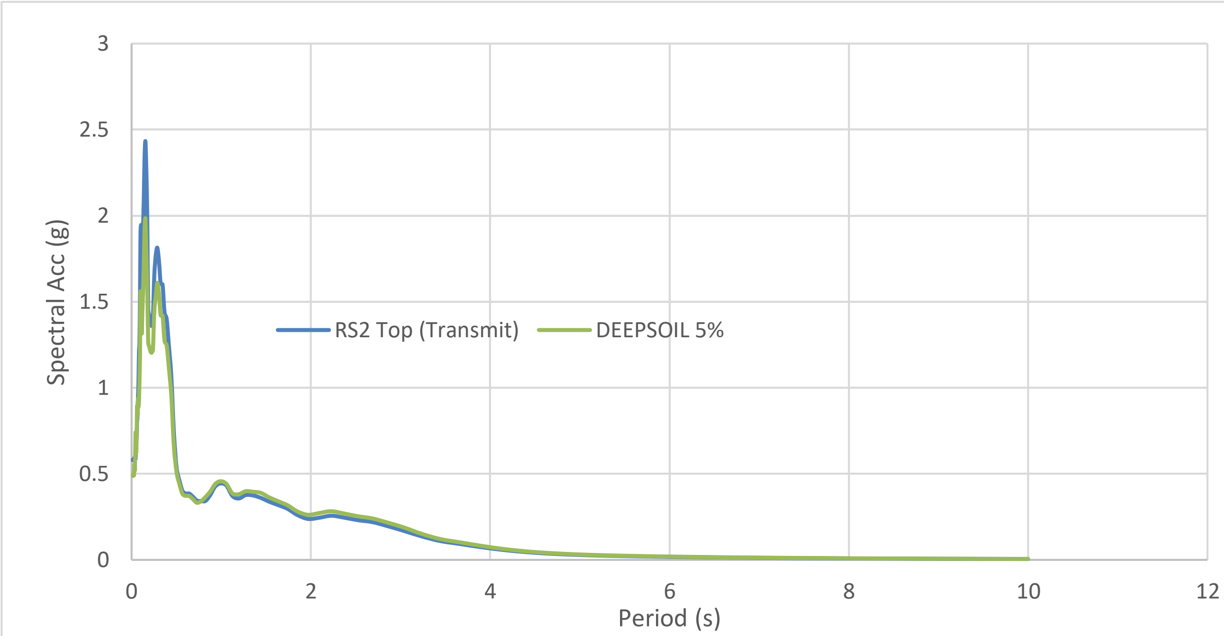

Figure 16-2: Ground Motion Velocity and Spectral Acceleration from RS2 Compared with DEEPSOIL

16.5 References

Itasca Consulting Group Inc. (2011). *FLAC version 7.0: Dynamic Analysis*.

Hashash, Y.M.A., Musgrove, M.I., Harmon, J.A., Groholski, D.R., Phillips, C.A., and Park, D. (2016) *"DEEPSOIL 6.1, User Manual".*

16.6 Data Files

The input data files **Dynamic #016.fez** and **Dynamic #016_Transmit.fez** can be downloaded from the RS2 Online Help page for Verification Manuals.

17 Free Field

17.1 Introduction

This verification is from FLAC example 1.4.1.4 Free-Field Boundaries:

Itasca Consulting Group Inc. (2011). FLAC Dynamic Analysis Version 7.0 (pp. 1.23 – 1.29).

In dynamic analysis, the material damping will absorb most of the energy in the waves reflected from distant boundaries. Therefore, *absorb* boundary is assigned to the base of the model and *transmit* boundary is assigned to the sides of the model to simulate the "leak out" effect of the wave energy of the sides. By applying these specific boundary conditions, free-field conditions are achieved.

17.2 Problem Description

The dynamic response of a model is simulated in RS2. A shear-stress wave is applied at the base and free-field boundaries are applied to the lateral boundary. The interest of this case is the horizontal displacement and velocity at different time queries. Figure **17-1** indicates the model geometry in RS2 and the numbers and locations of three different time queries. Figure **17-3** illustrates that the x-velocity results from RS2 and FLAC are almost identical.

17.3 Geometry and Properties

Table 17.1: Material Properties

ϕ′ (deg.)	E (kPa)	γ (kN/m^3)	υ
11	100000	0.025	0.25

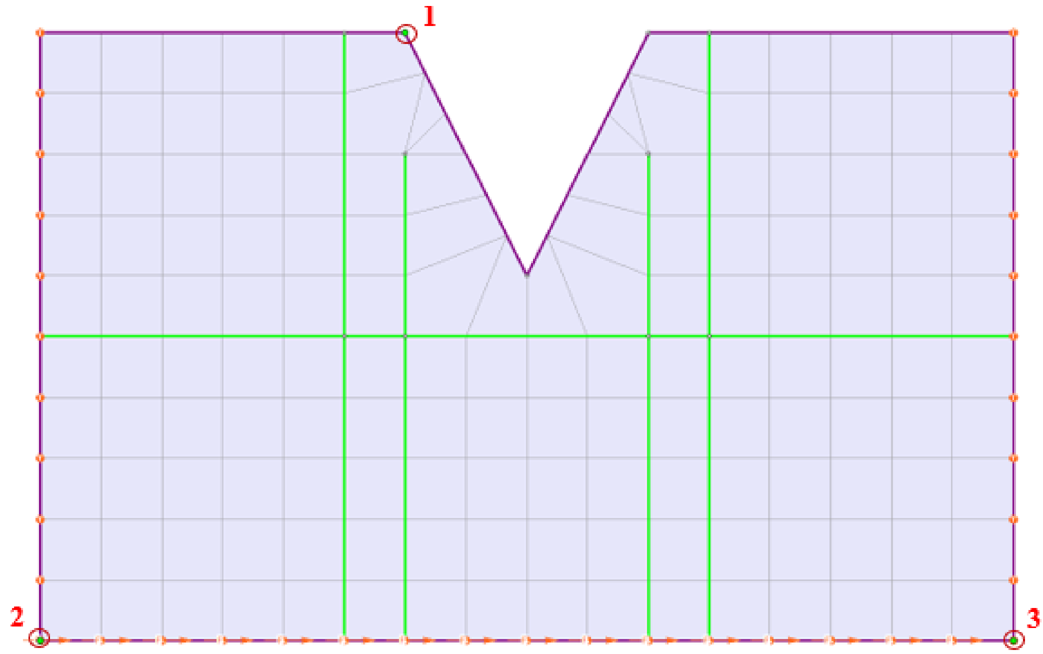

Figure 17-1: RS2 Model Geometry

17.4 Results

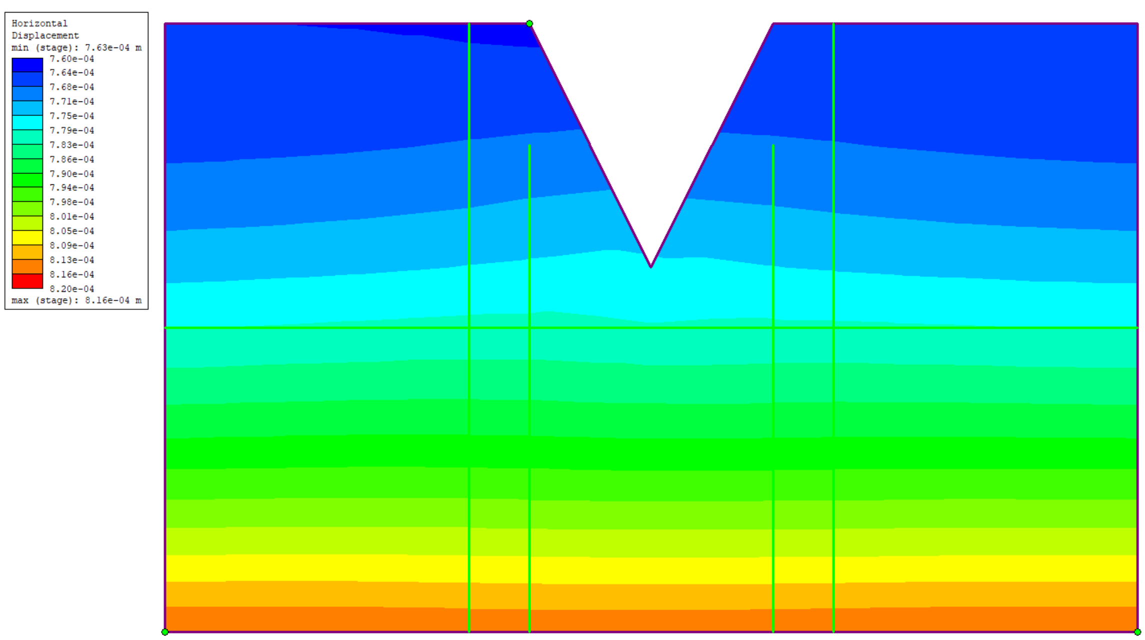

Figure 17-2: Example Horizontal Displacement Results in RS2

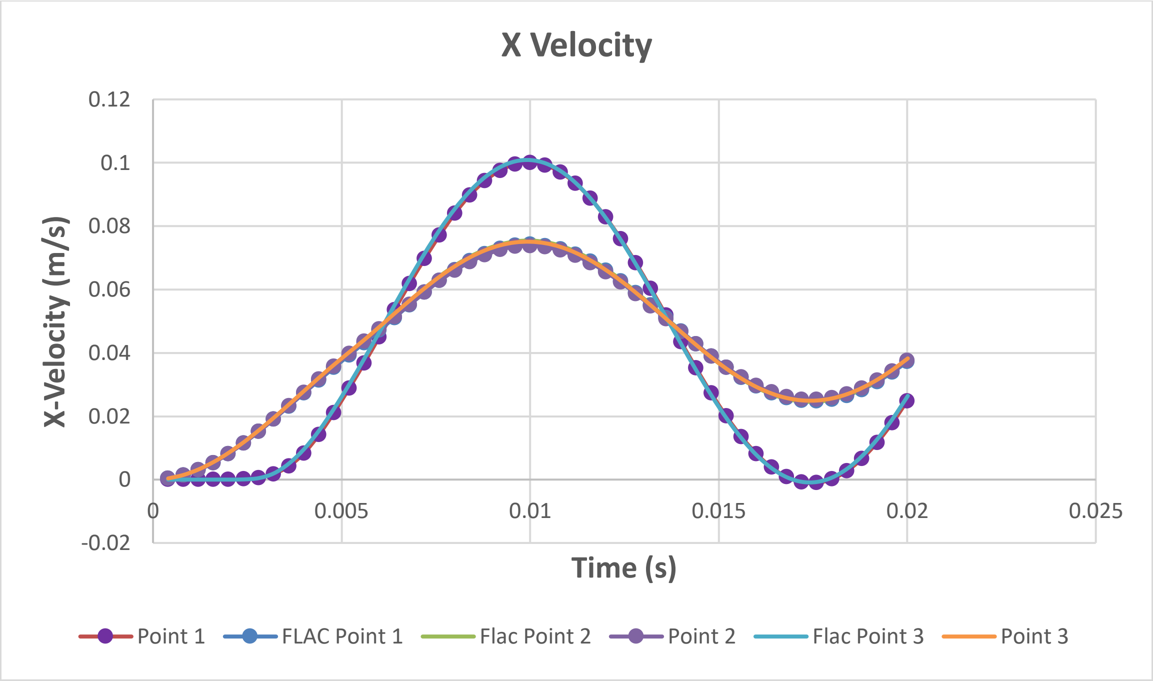

Figure 17-3: X-Velocity vs. Time at Different Time Queries

17.5 References

Itasca Consulting Group Inc. (2011). *FLAC version 7.0: Dynamic Analysis*.

17.6 Data Files

The input data file **Dynamic #017.fez** can be downloaded from the RS2 Online Help page for Verification Manuals.

18 Dynamic Pore-Pressure Generation

18.1 Introduction

This verification is from FLAC example 1.4.4 Dynamic Pore-Pressure Generation:

Itasca Consulting Group Inc. (2011). FLAC Dynamic Analysis Version 7.0 (pp. 105-120).

18.2 Background

Under rapid loading such as earthquake shaking, the pore pressure is increased and therefore the soil particles can readily move with respect to each other in saturated soil, causing a loss in the strength and stiffness of the soil. This phenomenon is defined as liquefaction. Particularly, when a saturated cohesionless soil is under rapid loading, the soil tends to densify, causing a reduce in the effective stress, which leads to liquefaction.

Although liquefaction is induced by the buildup in pore pressure under rapid loading, the direct cause of liquefaction is indeed the reduce in effective stress due to the decrease in contact forces between soil particles (Dinesh et al. 2004). Under repeated shear cycle, the soil grains are forced to rearranged continuously, which then may be forced to move up against the adjacent soil particles, leading to dilation of the soil. Therefore, dilation is an important element in the liquefaction process.

Liquefaction is expected where induced stresses exceed the soil resistance. In standard practice, a liquefaction analysis is performed on soil based on a total stress analysis in the following three steps to access the potential for liquefaction of the soils, assuming the liquefiable soil remains undrained at the in-situ void ratio (Byrne and Wijewickreme 2006).

1. Triggering of liquefaction: The cyclic stress ratio (CSR) determined from numerical simulation is compared to the cyclic resistance ratio (CRR) derived from empirical curves and the factor of safety against triggering liquefaction is determined.
2. Flow Slide Assessment: After the triggering analysis, zones that are predicted to liquefy are assigned with post-liquefaction (undrained) strengths, which can be analyzed from penetration resistance using empirical charts. A standard limit-equilibrium analysis is then performed to determine the factor of safety against a flow slide.
3. Seismic Displacements: In this step, the displacement of the potential sliding block of soil is predicted using the Newmark approach. The potential sliding block of soil is simulated as a rigid mass resting on an inclined plane. An acceleration is applied at the base to determine the displacement of the block caused by shaking.

The main concerns of this three-step approach are that the three steps are considered as separate steps even though there might be interaction locally in some zones of the soil structure, changing the overall behaviour of the soil mass. Moreover, the changes in pore pressure is not considered by this assessment.

In order to evaluate the pore pressure redistribution, four methods: total-stress synthesized procedure, loosely coupled effective-stress procedure, fully coupled effective-stress procedure and fully coupled effective-stress bounding-surface procedures can be used, depending on the material models of the soils.

Total-stress synthesized procedure derived by Beaty and Byrne (2000) combines the above three steps into one single analysis, the assumption of the undrained behaviour of the soil holds true. This procedure uses a total stress approach to liquefaction analysis and relied on the adjustment of liquefied element properties at the instant of triggering liquefaction.

Loosely coupled effective-stress procedure uses the Seed cyclic stress approach by Seed and Idrisis (1971) to generate pore pressure from shear stress cycles. This coupled effective-stress constitutive model measures the cyclic stress ratio (CSR) of each shear stress cycle to compute the incremental excessive pore pressure. The model counts shear stress cycles by tracking the shear stress acting on horizontal planes and looking for stress reversal and it incorporates residual strength by using a two-segment failure envelope consisting of a residual cohesion and zero friction angle that is extended to meet with the traditional Mohr-Coulomb failure envelope. The Finn model in RS2 is currently using this approach.

Fully coupled effective-stress procedure focuses on predicting seismic response and liquefaction of cohesionless soils in plan strains. The elasto-plastic model is based on a hyperbolic relation between stress ratio and plastic shear strain similar to Duncan and Chang (1970)'s, which is applicable to the *Manzari and Dafalias* model in RS2.

The last one, fully coupled effective-stress bounding-surface procedure provides the capability to consider cyclic stress reversal in two and three dimensions. This constitutive model can reproduce the behaviour of soil under cyclic loading, including the reduce in shear modulus, the increase of hysteretic damping with cyclic shear strain amplitude, the shear and volumetric strain accumulation at a decreasing rate as the numbers of cycle increases, and the increase in liquefaction resistance with density. This model is applicable to the *Bounding Surface Plasticity* model in RS2.

Finn Model Formulation

Since the primary effect of liquefaction is the irrecoverable volume contraction in the soil grains, meaning a change in volumetric strain, when the soil is under a strain cycle with constant confining stress. If the voids are filled with fluid, the pore pressure and effective pressure stay constant if the volume is constant; however, when there is a volume contraction, the pore pressure increases and the effective pressure decreases.

This independency of the volumetric strain and cyclic shear-strain amplitude with respect to confining stress is noted by Martin et al. (1975) defined this mechanism as the following empirical equation:

$$\Delta\epsilon_{vd} = C_1(\gamma - C_2\epsilon_{vd}) + \frac{C_3\epsilon_{vd}^2}{\gamma + C_4\epsilon_{vd}} \tag{1.1}$$

Where $\Delta\epsilon_{vd}$ is the cyclic shear-strain amplitude,

γ is the engineering shear strain,

$C_1, C_2, C_3, and\ C_4$ are constants equal to 0.8, 0.79, 0.45 and 0.73 respectively.

It should be noted that the equation takes account of the accumulated irrecoverable volume strain ϵ_{vd} by decreasing the increment in volume strain as the volume strain is accumulated. Presumably, $\Delta\epsilon_{vd}$ should be zero if γ is zero. Martins et al. also compute the change in pore pressure by assuming certain boundary conditions that were not clearly stated, which are taken care by RS2.

Another similar formula derived by Byrne (1991) also define this mechanism, in a simpler way:

$$\frac{\Delta\epsilon_{vd}}{\gamma} = C_1 exp\left(-C_2 \frac{\epsilon_{vd}}{\gamma C_1}\right) \tag{1.2}$$

Where $\Delta\epsilon_{vd}$ is the cyclic shear-strain amplitude,

γ is the engineering shear strain,

C_1, C_2 are constants, $C_1 = 7600(D_r)^2, C_2 = \frac{0.4}{C_1}$

Figure 18-1 illustrates the shear induced volumetric strain for constant amplitude of cyclic shear strain predicted by this formula. It can be shown from figure 1.1 that the formula predicts the volumetric strain to have an upward tendency with a decreasing rate of accumulation as the number of cycles grows.

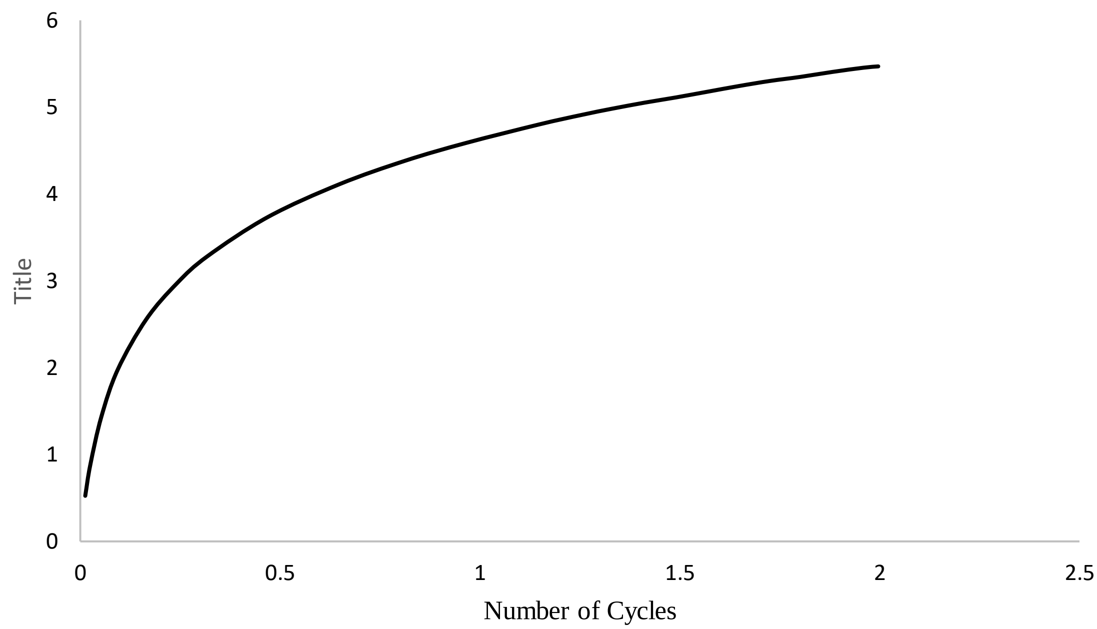

Figure 18-1: Byrne Formula Graph

The incremental volumetric behaviour of the Byrne model can be expressed as equation (1.3):

$$\Delta\sigma_m + \alpha\Delta p = K(\Delta\epsilon + \Delta\epsilon_{vd}) \qquad (1.3)$$

Where $\sigma_m = \sigma_{ii}/3$ is the mean stress,
P is pore pressure,
α is Biot coefficient (=1 for soil),
K is the drained bulk modulus of the soil,
ϵ is the volumetric strain.
For undrained conditions, the change in pore pressure is proportional to the change in volumetric strain as:

$$\Delta p = -\alpha M \Delta\epsilon \qquad (1.4)$$

Where M is Biot modulus. After substitution of Equation (1.4) into (1.3), and solving for $\Delta\epsilon$, the following equation can be obtained:

$$\Delta\epsilon = \frac{\Delta\sigma_m - K\Delta\epsilon_{vd}}{K + \alpha^2 M} \qquad (1.5)$$

If Equation (1.5) predicts no change in volume, then use $\Delta\epsilon = 0$ in Equation (1.3) gives us:

$$\Delta\sigma_m + \alpha\Delta p = K\Delta\epsilon_{vd} \qquad (1.6)$$

Equation (1.6) predicts a decrease in magnitude of effective stress with cyclic shear strain which is produced by an increase of shear induced compaction. Under conditions of constant stress, $\Delta\sigma_m = 0$, an increase in pore pressure can be observed:

$$\Delta p = K\Delta\epsilon_{vd} \tag{1.7}$$

The increase in pore pressure is proportional to the drained bulk modulus of the soil. While under free stress conditions, the pore pressure will remain unchanged ($\Delta p = 0$), and the magnitude of the total stress will decrease according to:

$$\Delta\sigma_m = K\Delta\epsilon_{vd} \tag{1.8}$$

Please note that in both situations, the drained bulk modulus, K, is essential in determining the magnitude of the cyclic loading impact on effective stress. Therefore, the Byrne model captures the important physics of liquefaction.

18.3 Problem Description

A shaking table model consist of a box of sand is simulated in RS2. Periodic motion is applied at the base, on the two sides of the box and diminishes to zero at the top. Gravity is the only vertical loading in this case. The stresses and pore pressure are computed using the Martin et al. (1975) and the Byrne (1991) formulas. The α, β and time step are adjusted in RS2 to match the dynamic analysis damping parameters defined in FLAC. Figure 1.1 indicates the model geometry in RS2 and the numbers and locations of three different time queries. Figures 1.3a and 1.3b illustrates that the predicted pore pressure at three different time queries using either Martin or Byrne formulas has similar trends, and that the pore pressure results from RS2 and FLAC are almost identical.

18.4 Geometry and Properties

Table 18.1: Material Properties

Analysis	φ′ (deg.)	E (kPa)	γ (kN/m^3)	C1	C2	C3	C4
Martin	35	491000	25.0	0.8	0.79	0.45	0.73
Byrne	35	491000	25.0	0.463234	0.431747	NA	NA

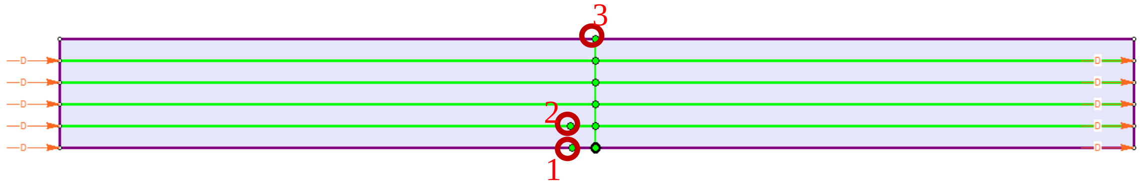

Figure 18-2: RS2 Model Geometry

18.5 Results

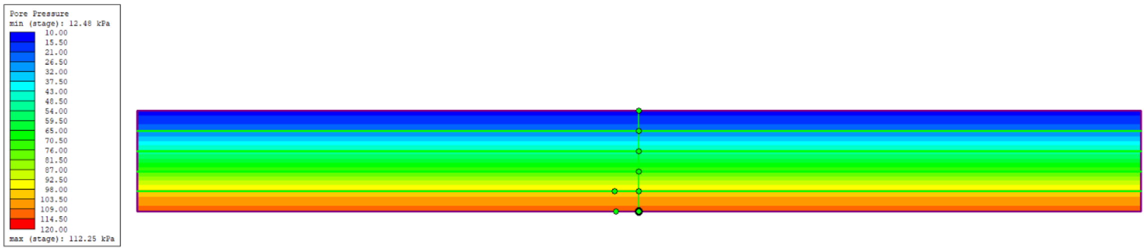

Figure 18-3: Example Pore Pressure Results in RS2 Using Byrne Formula

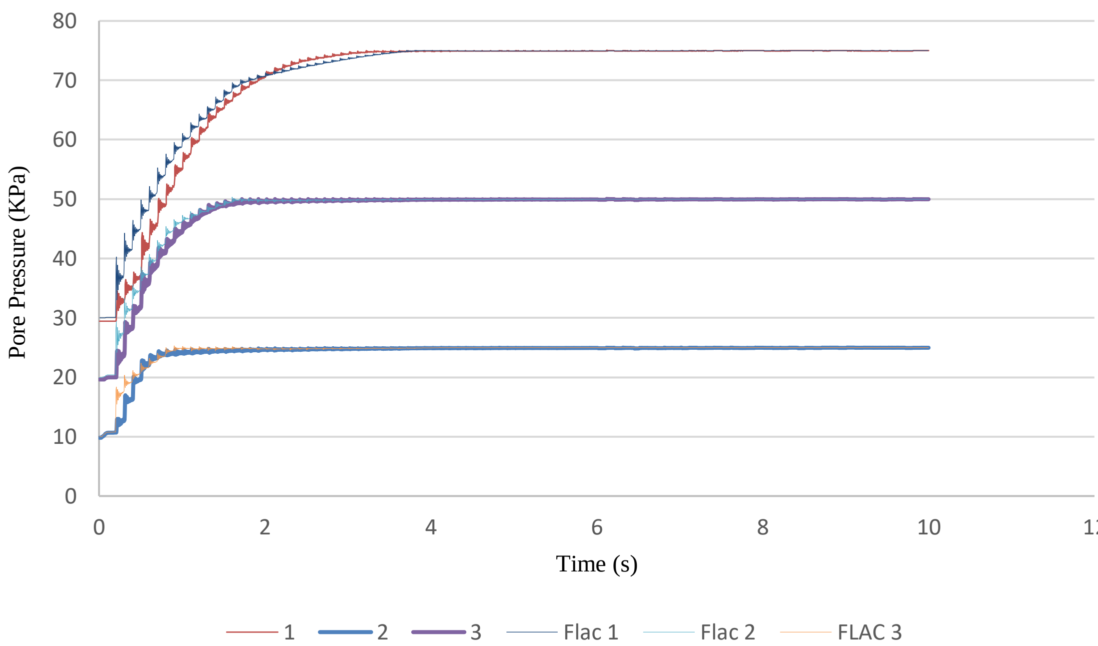

Figure 18-4: Pore Pressure vs. Time at Different Time Queries Using Martin Formula

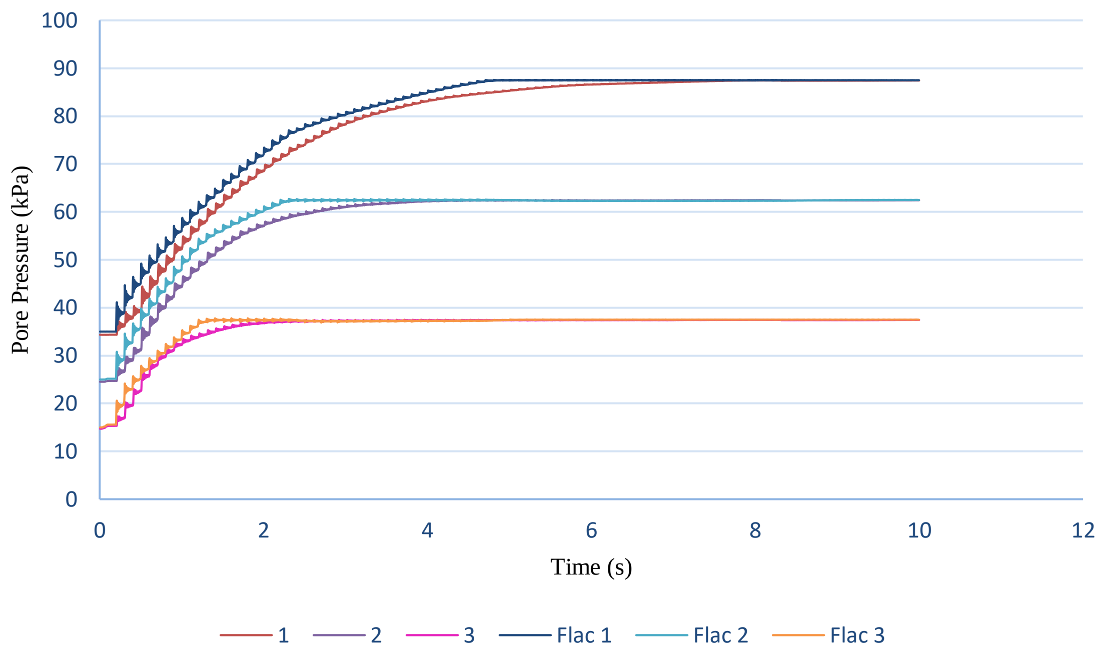

Figure 18-5: Pore Pressure vs. Time at Different Time Queries Using Byrne Formula

18.6 References

Beaty, M. H. & P. Byrne. (2000). *A synthesized approach for predicting liquefaction and resulting displacements.* In Proceedings of the Twelve World Conference on Earthquake Engineering, Auckland, New Zealand, Paper No. 1589, January 30 – February 4.

Byrne, P. M. & D. L. Anderson. (1991). *Earthquake Design in the Fraser Delta, Task Force Report*. City of Richmond, B.C. publication and Soil Mech. Series No. 150, Dept. of Civil Engineering, University of British Columbia, Vancouver, B.C.

Byrne, P. M. & D. Wijewickreme. (2006). *Liquefaction Resistance and Post-Liquefaction Response of Soils for Seismic Design of Buildings in Greater Vancouver.* Sea to Sky Geotechnique (59th Canadian Geotechnical Conference & 7th Joint CGS/IAH-CNC Groundwater Specialty Conference, Vancouver, Canada, October 2006), pp. 1267-1278.

Byrne, P.M. & McIntyre, J. (1994). *Deformations in granular soils due to cyclic loading.* In: Proceedings of Settlement 94, ASCE Geotechnical Special Publication No. 40, Texas, June, pp. 1864–1896.

Duncan, J. M. & C-Y. Chang. (1970). *Nonlinear Analysis of Stress and Strain in Soils.* Soil Mechanics, 96(SM5), 1629-1653.

Dinesh, S. V., T. G. Sitharam & J. S. Vinod. (2004). *Dynamic properties and liquefaction behavior of granular materials using discrete element method.* Current Science, Special Section: Geotechnics and earthquake hazards, Vol 87, No. 10.

Finn, W.D.L., Lee, K.W. & Martin, G.R. (1977). *An effective stress model for liquefaction*. J. Geotechnical Engineering Division, ASCE 103, 513–533.

Itasca Consulting Group Inc. (2011). *FLAC version 7.0: Dynamic Analysis*.

Seed, H.B., Lee, K.L., Idriss, I.M. & Makdisi, F.I. (1975). *The slides on the San Fernando dams during the earthquake of February 9, 1971*. J. Geotechnical Engineering Division, ASCE 101 (7), 651–688.

18.7 Data Files

The input data files **Dynamic #018_Byrne.fez** and **Dynamic #018_Martin.fez** can be downloaded from the RS2 Online Help page for Verification Manuals.